Deposition of the Devonian Bahram Formation in the Central-East Iranian microcontinent

Depósito de la Formación Bahram del Devónico en la parte Central-Este del microcontinente de Irán

Amir Hossein **Rahiminejad**[1,*], Hoda **Bavi**[2]

[1] Department of Ecology, Institute of Science and High Technology and Environmental Sciences, Graduate University of Advanced Technology, Kerman, Bagh-e-Alavi Highway Knowledge Paradise 26WX+R86 Kerman, Iran.

[2] Department of Geology, Faculty of Sciences, Shahid Bahonar University of Kerman, Pajoohesh Sq. 76169-14111, Kerman, Iran.

* Corresponding author:
(A.H. Rahiminejad) *ah.rahiminejad@kgut.ac.ir*

How to cite this article:
Rahiminejad, A.H., Bavi, H., Deposition of the Devonian Bahram Formation in the Central-East Iranian microcontinent: Boletín de la Sociedad Geológica Mexicana, 77(2), A060625. http://dx.doi.org/10.18268/BSGM2025v77n2a060625

Manuscript received: April 28, 2025
Corrected manuscript received: May 25, 2025
Manuscript accepted: June 3, 2025

Peer Reviewing under the responsibility of Universidad Nacional Autónoma de México.

ABSTRACT

During the Middle-Late Devonian, the Bahram Formation was deposited in the northern margin of the Gondwana. The formation was mainly precipitated on a homoclinal carbonate ramp in the central Iran and the Central-East Iranian Microcontinent (CEIM). Our studies on a mixed carbonate-clastic succession in the north of the Kerman area, south of the CEIM indicate that the Bahram Formation comprises two clastic and seven carbonate facies representing tidal flat, back-reef lagoon and coral-stromatoporoid marginal reef paleoenvironments. The identified facies and paleoenvironments point to development of a mixed carbonate-clastic shallow marine rimmed shelf during the Middle-Late Devonian. Generally, due to a shallow-trend and a gradual increase in inputs of clastic sediments from the continental environments along a direction from the northern parts of the CEIM towards its southern parts and the central Iran, mixed carbonate-clastic shallow marine depositional systems of the Bahram Formation were developed. Reefal and biostromal shoals/barriers of the inner and middle ramps and/or shelves of the formation were also extended along the same shallowing-trend. This study introduces a rare sedimentary model for the Bahram Formation's depositional system in the northern Kerman area, contributing to broader investigations of Devonian mixed carbonate-clastic systems and paleoenvironmental dynamics on Gondwana's northern margin.

Keywords: Bahram Formation, Iran, Devonian, mixed carbonate-clastic shelf, facies analysis, paleoenvironment.

RESUMEN

Durante el Devónico Medio-Tardío, la Formación Bahram fue depositada en el margen norte de Gondwana. Esta formación fue precipitada principalmente en una rampa carbonatada homoclinal en Irán central y el Microcontinente Centro-Este de Irán (MCEI). Nuestros estudios en la sucesión mixta carbonatada-clástica en el área norte de Kerman, al sur del MCEI, indican que la Formación Bahram comprende dos facies clásticas y siete facies carbonatadas, representando planicie mareal, laguna posterior de arrecife y paleoambientes marginales de arrecifes coral-estromatopóridos. Las facies y paleoambientes identificados apuntan al desarrollo de una plataforma marina restringida, mixta carbonato-clástica, durante el Devónico Medio-Tardío. Esta plataforma de la Formación Bahram se desarrolló debido a una tendencia hacia aguas someras y un gradual incremento en el aporte de sedimentos clásticos de los ambientes continentales a lo largo de una dirección de la porción norte del MCEI, desde sus porciones del norte hacia sus porciones central y sur y el centro de Irán. Barreras de naturaleza arrecifal y de biostromas someros en las rampas interna y media de la formación, se extendieron también a lo largo de la tendencia hacia la somerización. Este estudio presenta un modelo sedimentario poco común para el sistema de depósito de la Formación Bahram en el área norte de Kerman, contribuyendo a investigaciones más amplias sobre sistemas mixtos carbonato-clástico del Devónico y las dinámicas paleoambientales en el margen norte de Gondwana.

Palabras clave: formación Bahram, Irán, Devónico, plataforma mixta carbonato-clástica, análisis de facies, paleoambiente.

http://dx.doi.org/10.18268/BSGM2025v77n2a060625

1. Introduction

Mixed carbonate-siliciclastic/clastic systems and/or successions are diverse in both ancient and modern shallow-marine settings (Wilson and Lokier, 2002; Lubeseder *et al.*, 2009; Ferronatto *et al.*, 2021). These represent a transition between carbonate and clastic sedimentation and partially consist of both siliciclasts/clastic and in situ calcareous components (Mount, 1984, 1985; Chiarella *et al.*, 2012; Chiarella and Longhitano, 2012; Zecchin and Catuneanu, 2017; Sorci *et al.*, 2023). Ancient mixed carbonate-clastic successions and settings provide significant insights into paleoclimatic, paleogeographic and paleo-depositional changes during the past (Lubeseder *et al.*, 2009; Wei *et al.*, 2021; Sorci *et al.*, 2023).

The Middle-Upper Devonian Bahram Formation in the north of the Kerman area in the south of the Central-East Iranian Microcontinent is an excellent example of mixed carbonate-clastic successions/systems in the Iran Plate (*e.g.*, Hashmie *et al.*, 2016). Generally, the Bahram Formation comprises both carbonate and clastic deposits (Wendt *et al.*, 2002; Aghanabati, 2004). The carbonate deposits of the formation are rich in marine fossil invertebrates such as brachiopods (dominant), tabulate and rugose corals, stromatoporoids, tentaculitids, bryozoans, crinoids, conodonts, sparse molluscs and trilobites (Wendt *et al.*, 2002; Zamani *et al.*, 2021). Lithologically, the Bahram Formation with a thickness between 100m to more than 300m consists mainly of limestone, dolomitic limestone and intercalations of shale and sandstone (Wendt *et al.*, 2002; Aghanabati, 2004; Ghorbani, 2019).

However, the lithology, facies, thickness and the accurate age of the Bahram Formation and its equivalents are variable in the Central-East Iranian Microcontinent (CEIM), central, and the northern parts of Iran, where they were deposited (Wendt *et al.*, 2002, 2005; Hashmie *et al.*, 2016; Salehi *et al.*, 2020). Generally, deposition of the Bahram Formation generally took place during the Givetian (Middle Devonian)-Famennian (Late Devonian) (Wendt *et al.*, 2002; Aghanabati, 2004; Bahrami *et al.*, 2015; Zamani *et al.*, 2021).

Most of the studies carried out on the Bahram Formation were focused on the biostratigraphic analyses (*e.g.*, Gholamalian, 2006; Ahmadi *et al.*, 2012; Bahrami *et al.*, 2014, 2015; Gholamalian *et al.*, 2015; Zamani *et al.*, 2021). Detailed stratigraphic, paleoenvironmental and facies aspects of the Devonian mixed carbonate-clastic systems /settings of the Bahram Formation are poorly known and not well documented in the literature. Although some related studies were carried out by Hashmie *et al.* (2016), Königshof *et al.* (2017) and Hassani *et al.* (2020). However, significant researches on detailed stratigraphic and sedimentological aspects of the carbonate sequences and facies of the Bahram Formation have been published in the international journals by Wendt *et al.* (1997), Wendt *et al.* (2002), Hoseinabadi *et al.* (2016), Königshof *et al.* (2017) and Salehi *et al.* (2020).

This paper is focused on detailed stratigraphic and facies analyses of a Middle-Upper Devonian mixed carbonate-clastic succession of the Bahram Formation in the south of the Central-East Iranian Microcontinent and reconstruction of the depositional model of the formation. Our studies contribute to a better understanding of types and formation of ancient mixed carbonate-clastic systems and paleoenvironmental and depositional changes during the Devonian in the north of the Gondwana.

2. Geological setting and locality of the studied succession

Generally, the Iran Plate is composed of a number of tectonic and structural zones comprising central Iran, the Central-East Iranian Microcontinent, NW Iran and the Binalud and Alborz Mountains (Figure 1a; Takin, 1972; Zand-Moghadam *et al.*, 2014; Salehi *et al.*, 2020). The Devonian deposits of the Bahram Formation are well exposed in the central Iran and the Central-East Iranian

http://dx.doi.org/10.18268/BSGM2025v77n2a060625

Microcontinent (*e.g.*, Ahmadi *et al.*, 2012; Bahrami *et al.*, 2015; Hashmie *et al.*, 2016; Hoseinabadi *et al.*, 2016; Salehi *et al.* 2020; Zamani *et al.*, 2021). The Central-East Iranian Microcontinent consists of the three north-south trending Lut, Tabas and Yazd structural blocks (Figure 1a; Stöcklin, 1968, 1977; Hashmie *et al.*, 2016). This Devonian deposits are best exposed in the Tabas Block and the north of the Kerman area in the south of the block (Wendt *et al.*, 2002; Hashmie *et al.*, 2016).

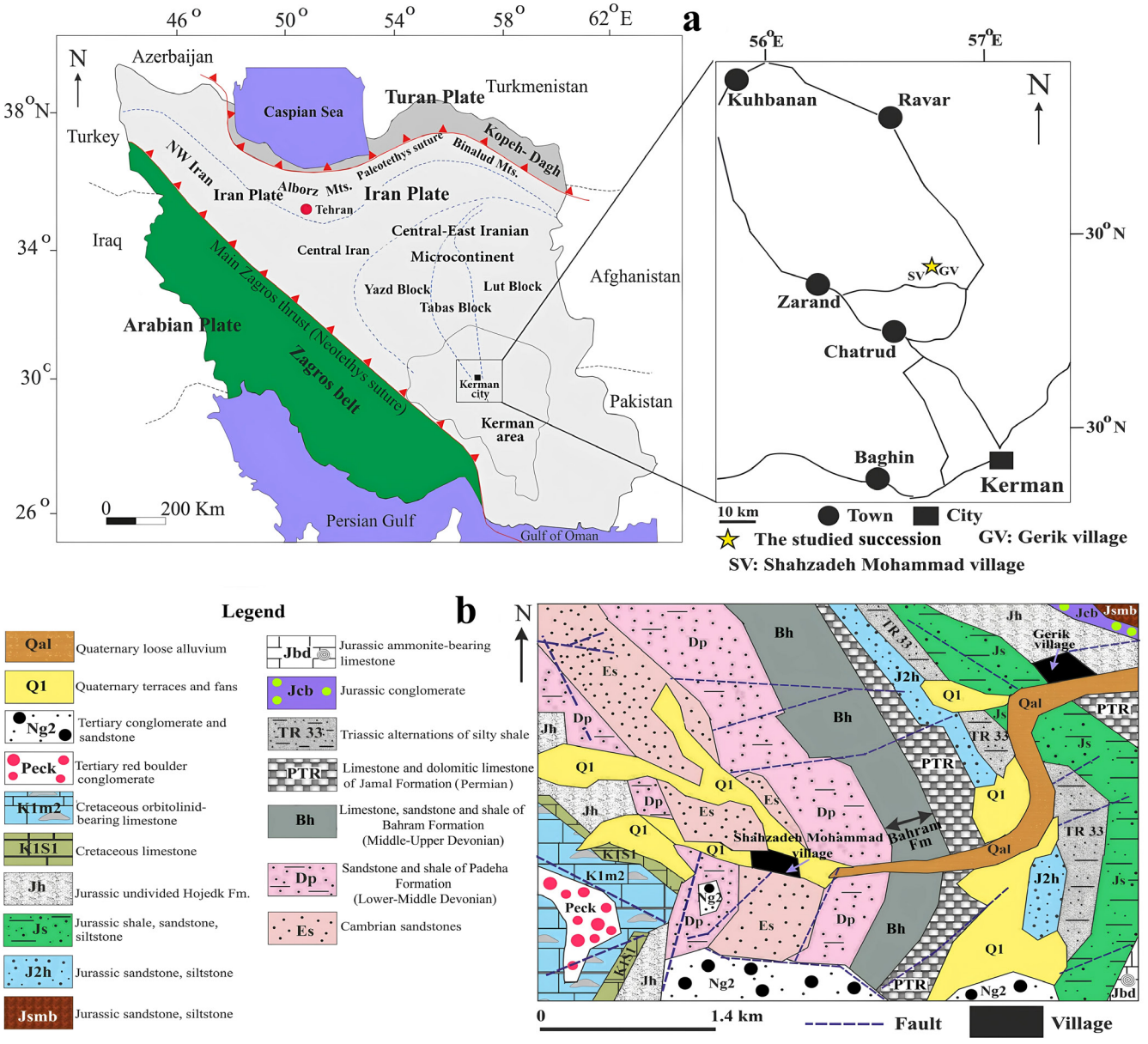

Figure 1 a) The structural map of the Iran Plate and location of the studied stratigraphic succession of the Middle-Upper Devonian Bahram Formation in the north of the Kerman area. The studied succession of the formation is located in the south of the Tabas Block in the south of the Central-East Iranian Microcontinent. The succession is situated between the Shahzadeh Mohammad and Gerik villages (modified and redrawn from Wilmsen *et al.*, 2009; Rahiminejad and Zand-Moghadam, 2018; Zamani *et al.*, 2021), b) Geological map of the area in the north of the Kerman area, near the studied succession in the north of the city of Kerman (modified and redrawn from Vahdati-Daneshmand *et al.*, 1995 and Zamani *et al.*, 2021). Db, Dcsh, Ds2 and b are representative of the deposits of the Bahram Formation.

http://dx.doi.org/10.18268/BSGM2025v77n2a060625

The Tabas Block was formed in a foreland basin comprising a thick succession of carbonate and clastic rocks (Wendt *et al.*, 2002) in the central part of the Central-East Iranian Microcontinent (Takin, 1972; Stöcklin, 1974).

In this study, the selected succession of the Bahram Formation in the north of the Kerman area is located in the south of the Tabas Block, south of the Central-East Iranian Microcontinent (Figures 1-3). The succession is situated between the villages of Gerik and Shahzadeh Mohammad about 60 km north of the city of Kerman and about 30 km east of Zarand (Figure 1).

The coordinates of the base of the succession are 30°48′19.74″ N and 56°56′3.45″ E. The coordinates of the top of the succession are 30°48′21.77″N and 56°56′17.03″E. In the area near the studied succession, the exposed deposits include Cambrian sandstones, sandstones and shales of the Lower-Middle Devonian Padeha Formation, limestones, shales and sandstones of the Middle-Upper Devonian Bahram Formation, limestone and dolomitic limestone of the Permian Jamal Formation, Triassic silty shales, Jurassic rocks (shales, sandstones, siltstones, ammonite-bearing limestones and conglomerates), undivided Jurassic Hojedk Formation, Cretaceous limestones, Cretaceous orbitolinid and rudist-bearing limestones, Tertiary conglomerates and sandstones and Quaternary terraces, fans and alluvium (Figure 1b; Vahdati-Daneshmand *et al.*, 1995). Based on the conodont biozonation used by Zamani *et al.* (2021), the age of the Bahram Formation in this study ranges from Givetian (Middle Devonian) to Famennian (Latest Devonian; Figure 2).

3. Materials and methods

The stratigraphic succession of the Bahram Formation was selected based on the geological map of Zarand compiled by Vahdati-Daneshmand *et al.* (1995). The stratigraphic features (thickness, lithology, sedimentary structures) and macrofossil content of the strata of the Bahram Formation were measured and recorded during the fieldwork.

A total of 130 rock samples (carbonate, sandstone, and shale) were collected from the formation. Thin-sections were prepared from the carbonate rock samples and sandstones for microscopic analyses and petrographic studies. The thin-sections were analyzed with a transmitting microscope Nikon model BK POOL, an Olympus Polarizing Microscope model BH-2 and a Yaxun Ak-21 Binocular Stereo Microscope. Facies of carbonate rocks and sandstones were studied and identified during the fieldwork and microscopic analyses of the thin-sections. The type, size, and abundance of sedimentary grains and the texture and composition of the groundmass of the carbonate and sandstone facies were evaluated during microscopic examination of the thin-sections. The staining method of Dickson (1966) was used to identify dolomite grains in the carbonate rocks. A mixture of 100 ml of hydrochloric acid (1.5%) and 0.2 g of Alizarin Red S was prepared. The thin-sections of the carbonate rocks were kept in the mixed solution for about 20 seconds. The dolomite minerals in the thin-sections remained colourless.

However, the calcite minerals turned red. Shales facies were studied and described based on field observations. Nevertheless, some shale samples were washed and sieved and the obtained loose sedimentary materials were studied by a binocular microscope in order to investigate the type of the sedimentary grains. The study and classification of the carbonate facies is based on Dunham (1962) and Embry and Klovan (1971). The texture of the sandstone facies is classified according to Folk (1980).

4. Results

4.1. LITHOSTRATIGRAPHY

The studied succession of the Bahram Formation with a thickness of 274 m unconformably overlies the red clastic deposits (shales and sandstones) of the Lower-Middle Devonian Padeha Formation (Figures 2, 3a and 3b). The boundary between

http://dx.doi.org/10.18268/BSGM2025v77n2a060625

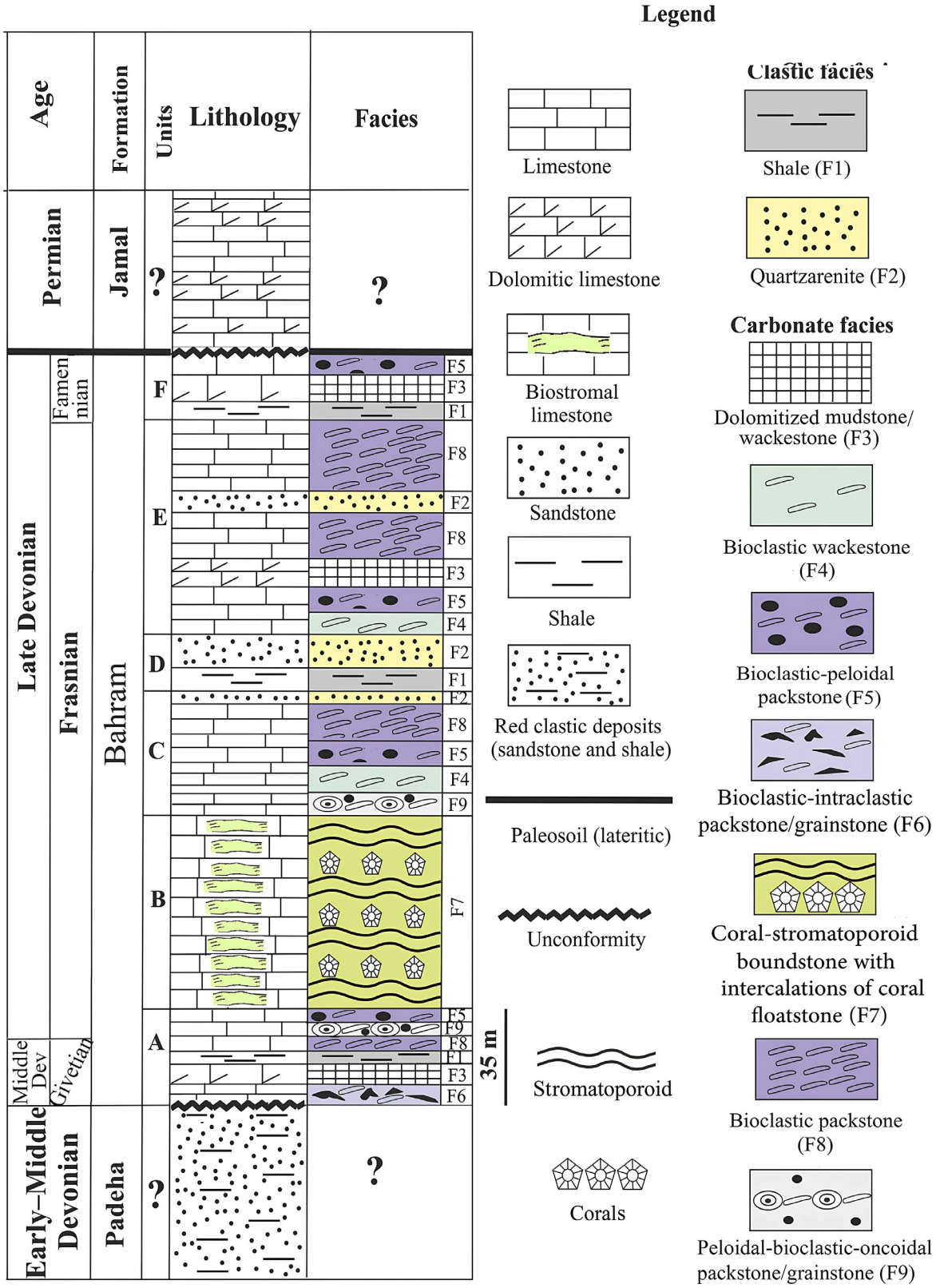

Figure 2 The stratigraphic succession of the Bahram Formation in the studied area. The age of the Bahram Formation in the studied succession is based on Zamani *et al.* (2021).

http://dx.doi.org/10.18268/BSGM2025v77n2a060625

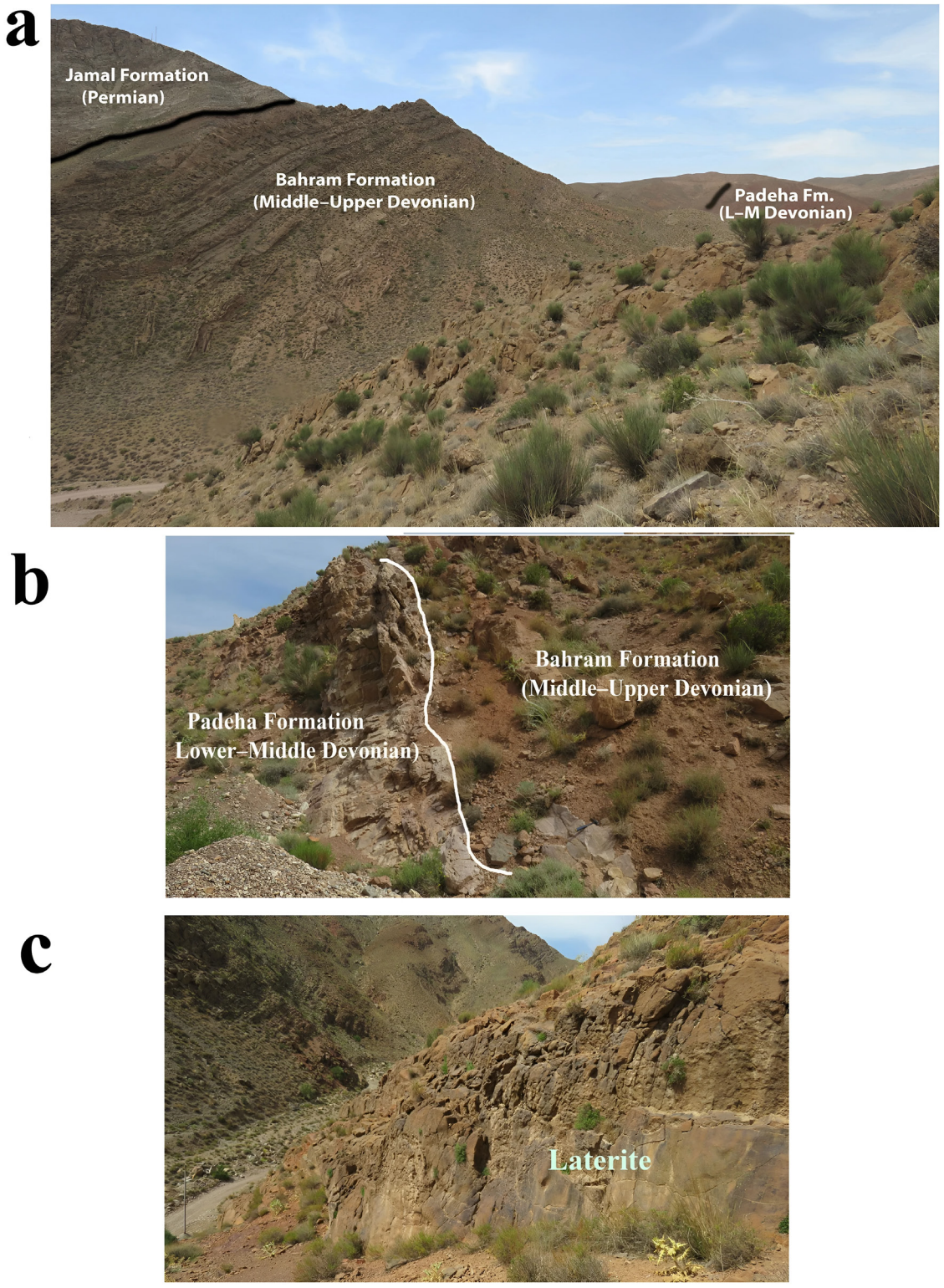

Figure 3 a) Outcrop view of the studied succession of the Bahram Formation in the north of the city of Kerman, b) The exposure of the erosional and unconformable boundary between the clastic deposits of the Lower-Middle Devonian Padeha Formation and the carbonate deposits of the Middle-Upper Devonian Bahram Formation in the studied succession, c) The boundary between the Devonian Bahram Formation and the Permian carbonate succession of the Jamal Formations is erosional and unconformable and is indicated by a paleosoil/lateritic interval.

http://dx.doi.org/10.18268/BSGM2025v77n2a060625

the two formations is erosional. The Bahram Formation is overlain by the Permian limestone and dolomitic limestone of the Jamal Formation (Figures 2 and 3a). The boundary between the Bahram and Jamal formations is erosional and is indicated by a paleosoil/lateritic interval (Figures 2, 3a and 3c).

In the studied succession, the Bahram Formation is informally divided into six lithostratigraphic units (see units A-F; Figure 2) from base to top: (1) Unit A with a thickness of 35 m consists of limestones in the lower and upper parts and dolomitic limestone and an interval of shale in the middle part. The limestones contain brown, large calcareous angular debris and pebbles. Oncoids are present in the upper part of Unit A. (2) Unit B is composed of a 70 m-thick interval of biostromal limestone. The interval is continuous and laterally extends in the studied area between the villages of Gerik and Shahzadeh Mohammad in the north of the city of Kerman. (3) Unit C with a thickness of 45 m comprises yellow thin to thick-bedded limestone. Oncoids are present in the lower part of the unit. (4) Unit D is composed of a 21 m thick interval of clastic deposits. The lower part of Unit D comprises shale, whereas the upper part consists of sandstone. (5) Unit E (78 m thick) consists of limestone intercalated with intervals of sandstone and dolomitic limestone. (6) Unit F with a thickness of 25 m comprises shale, dolomitic limestone and limestone in the lower, middle and upper parts, respectively.

Generally, the sandstones in the studied succession of the Bahram Formation crop out as thin to medium-bedded intervals and display horizontal and cross beddings. The limestones in the succession are exposed as thin to thick-bedded intervals. The dominant well-preserved macrofossils in the limestones include brachiopods, corals and stromatoporoids. Bryozoans and echinoderms are the subordinate macrofossils in the limestones. The thick interval of biostromal limestone in Unit B of the Bahram Formation (Figure 2) is dominated by corals and stromatoporoids.

4.2. FACIES TYPES

Nine facies were identified in the studied succession of the Bahram Formation (Figures 2, 4-8 and Table 1). The distribution of the facies in the lithostratigraphic units of the formation is shown in Figure 2. The identified clastic facies include shale (F1) and sandstone (quartzarenite: F2). The carbonate facies are: dolomitized mudstone/wackestone (F3), bioclastic wackestone (F4), bioclastic-peloidal packstone (F5), bioclastic-intraclastic packstone/grainstone (F6), coral-stromatoporoid boundstone with intercalations of coral floatstone (F7), bioclastic packstone (F8) and peloidal-bioclastic-oncoidal packstone/grainstone (F9). The facies are described as follows:

4.2.1. FACIES F1: SHALE

Facies F1 comprises green and dark grey shales. Stratigraphically, the shale facies (Figure 4a) in the studied succession, is intercalated with both sandstone (F2) and carbonate facies (Figure 2). Dolomitized mudstone/wackestone (facies F3) and bioclastic packstone (facies F8) are the carbonate facies deposited directly above or below the shale facies-bearing intervals in the succession (Figure 2). Fine-grained detrital quartz grains and bioclasts or skeletal fragments of shallow marine benthic invertebrates are scattered in facies F1.

4.2.2. FACIES F2: QUARTZARENITE

This grain-supported and supermature sandstone facies (Figure 4b) is dominated by monocrystalline quartz grains (95%). Subordinately, polycrystalline quartz grains are also present (5%). Generally, the quartz grains in facies F2 range in size from about 0.3 to 0.5 mm. The grains are subrounded and well-sorted. Body fossils including skeletal fragments or bioclasts are absent in the facies. Facies F2 is dominated in the sandstone-bearing intervals (Figure 2) in the studied succession. The sandstone-bearing intervals display horizontal and cross beddings. Trace fossils of the ichnogenus Skolithos are abundant in the sandstone-bearing

Table 1. Facies types, their main sedimentary and stratigraphic features and the paleoenvironments of the Bahram Formation (Givetian-Famennian) in the studied succession. The depositional model of the Bahram Formation is consistent with a mixed carbonate-clastic shallow marine rimmed shelf. The reef front zone of the reef paleoenvironment was established on the middle shelf, whereas the tidal flat and back-reef lagoon paleoenvironments and the reef crest zone of the reef paleoenvironment were developed on the inner shelf.

Facies	The main sedimentary and stratigraphic features of the facies	Paleoenvironments on a mixed carbonate-clastic shallow marine rimmed shelf
Shale (F1)	1–Green and dark grey shales intercalated with sandstone (F2) and carbonate facies (F3 and F8) 2–Fine-grained detrital quartz grains and bioclasts of shallow marine benthic invertebrates are scattered in the shale facies.	Tidal flat: 1–subtidal zone
Quartzarenite (F2)	1–Grain-supported and supermature. 2–Main components: monocrystalline and sub-rounded and well-sorted quartz grains (95%). 3–Sedimentary structures: horizontal and cross beddings and abundant trace fossils such as *Skolithos*	Tidal flat: 1– supratidal zone to intertidal zone
Dolomitized mudstone/wackestone (F3): F3a: Unfossiliferous mudstone F3b: Fossiliferous wackestone	1– Texture: unfossiliferous mudstone and fossiliferous wackestone. 2–Dominated by: dolomites. 3– Subordinate allochems: sparse detrital quartz in the mudstone texture. Scattered and reworked bioclasts of shallow marine benthic invertebrates (brachiopods) in the fossiliferous wackestone texture.	Tidal flat: 1–supratidal zone to intertidal zone (with facies F3a) 2–subtidal zone (with facies F3b)
Bioclastic wackestone (F4)	1–Groundmass: micrite. 2–Main allochems: bioclasts of brachiopods, ostracods, bivalves and calcareous algae (80%). 3–Subordinate allochems: peloids and detrital quartz grains (20%). 4–Rare well-preserved fossil specimens of brachiopods with low diversity were observed in the outcrops of facies F4.	Back-reef lagoon (near tidal flat)
Bioclastic-peloidal packstone (F5)	1–Grain-supported. 2–Groundmass: micrite. 3–Main allochems: peloids (60%). 4–Subordinate allochems: bioclasts of bivalves (5%), echinoderms (10%) and brachiopods (25%). 5–Well-preserved fossil specimens of marine benthic invertebrates (mainly brachiopods) with low diversity were observed in the outcrops of facies F5.	Back-reef lagoon
Bioclastic-intraclastic packstone/grainstone (F6)	1–Grain-supported. 2–Groundmass: microsparite/sparite. 3–Main allochems: carbonate intraclasts commonly micritized and sub-rounded in shape (60%). 4–Subordinate allochems: bioclasts of brachiopods (35%) and very rare peloids (5%).	Tidal flat: 1–tidal channels connecting with back-reef lagoon
Coral-stromatoporoid boundstone with intercalations of coral floatstone (F7)	1–Dominated by abundant stromatoporoids, colonial hexagonarid - rugose corals and solitary rugose corals. 2–Forming a rigid carbonate framework in a 70m-thick interval of biostromal limestone. 3–Dominated by boundstone texture intercalated with floatstone texture. 4–Main components of the boundstone texture: colonial hexagonarid - rugose corals with cerioid massive growth form and stromatoporoids with both laminar and dome-shaped growth forms. 5–Main components of the floatstone texture: solitary rugose corals in a micritic groundmass. Solitary corals occasionally co-occur with stromatoporoids with laminar growth form and bryozoans.	Coral- stromatoporoid marginal reef: 1–reef crest zone (with boundstone facies) 2–reef front zone (with floatstone facies)
Bioclastic packstone (F8)	1–Grain-supported. 2–Groundmass: microsparite/sparite. 3–Allochems: bioclasts of echinoderms (50%), brachiopods (45%) and bivalves (5%). A number of the bioclasts are encrusted by micritic envelopes.	Tidal flat: 1–tidal channels connecting with back-reef lagoon
Peloidal-bioclastic-oncoidal packstone/grainstone (F9)	1–Grain-supported. 2–Groundmass: micrite (70%) and sparite (30%). 3–Allochems: Oncoids (50%), bioclasts of marine benthic invertebrates (30%) and peloids (20%). Main bioclasts: fragments of bryozoans and stromatoporoids. 4–Oncoids: elongated (with nucleus), spherical and subspherical (with or without nucleus) in shape. Nucleus of oncoids: fragments of bryozoans and other bioclasts. 5–Stratigraphically, the oncoid-bearing facies is deposited near a 70m-thick interval of biostromal limestone (with boundstone and floatstone textures) in the studied succession.	Back reef lagoon: 1– near marginal reef

http://dx.doi.org/10.18268/BSGM2025v77n2a060625

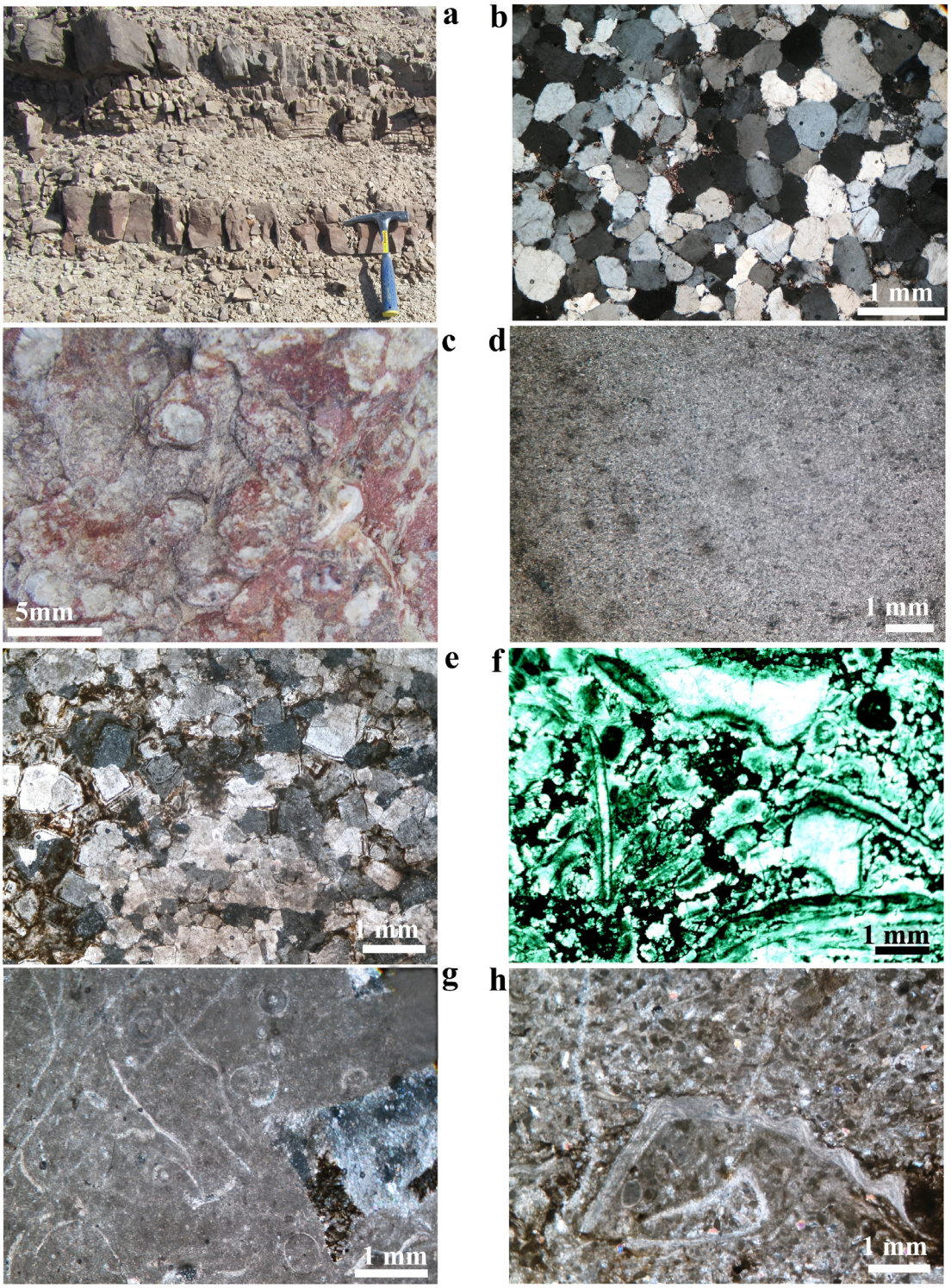

Figure 4 The identified facies in the studied succession of the Middle-Upper Devonian Bahram Formation, a) Outcrop view of the shale facies (F1), b and d–h) Thin-section microphotographs of the studied facies, b) Quartzarenite (F2), c) Field photo of trace fossils of the ichnogenus Skolithos on the rock surface of facies F2 in a sandstone-bearing interval, d–f) Dolomitized mudstone/wackestone (F3), d) Dolomitized mudstone (F3a: unfossiliferous mudstone). The mudstone texture of facies F3a is mainly occupied by fine-grained dolomites, e) Coarse-grained dolomites in the mudstone texture of facies F3a, f) Dolomitized wackestone (F3b: fossiliferous wackestone). Bioclasts or skeletal fragments of shallow marine benthic invertebrates are distributed in the wackestone texture of facies F3b, g) Bioclastic wackestone (F4), h) Bioclastic-peloidal packstone (F5).

intervals and/or the outcrops of facies F2 (Figure 4c).

4.2.3. FACIES F3: DOLOMITIZED MUDSTONE/ WACKESTONE

Facies F3 (Figures 4d, 4e, 4f and Table 1) is composed of an intensively dolomitized muddy/ micritic groundmass. Microscopic studies indicate that the primary texture of the facies ranges from unfossiliferous mudstone to fossiliferous wackestone (facies F3a and F3b; Figures 4d, 4e, 4f and Table 1). Both fine-grained and coarse-grained dolomites are present in facies F3 (Figures 4d and 4e). However, the fine-grained dolomites occupy about 70% of the unfossiliferous mudstone texture (Figure 4d). The coarse-grained dolomites (Figure 4e) occupy about 20% of the unfossiliferous mudstone texture and are commonly euhedral, and display zoning patterns. Fossils including bioclasts or skeletal fragments are absent in the unfossiliferous mudstone texture (F3a) of facies F3. Sparse detrital quartz grains are scattered in the mudstone texture of facies F3 (F3a). The wackestone texture of facies F3 is occupied mainly by medium and coarse-grained dolomites and is fossiliferous (F3b: fossiliferous wackestone). Reworked bioclasts or skeletal fragments of shallow marine benthic invertebrates (brachiopods) are scattered in the fossiliferous wackestone texture of facies F3 (Figure 4f). The bioclasts range in size from 2 to 7 mm.

4.2.4. FACIES F4: BIOCLASTIC WACKESTONE

Microscopic studies indicate that facies F4 consists of a micritic groundmass. Rare bioclasts of marine benthic invertebrates are the main grains or allochems in the facies, which are scattered and embedded in the groundmass (Figure 4g). The bioclasts (80% of the grains) mainly consist of fragments of brachiopods, ostracods, bivalves and calcareous algae. The bioclasts range in size from 0.5 to 2 mm. Peloids (0.1 to 0.4 mm in size) and detrital quartz grains are subordinately (20% of the grains) present in the facies.

Rare well-preserved fossil specimens of brachiopods with low diversity were observed in the outcrops of facies F4.

4.2.5. FACIES F5: BIOCLASTIC-PELOIDAL PACKSTONE

Based on microscopic studies, facies F5 contains bioclasts of marine benthic invertebrates and peloids which are embedded and densely packed in a packstone texture with a micritic groundmass (Figure 4h). The peloids are the most abundant grains or allochems (60% of the grains) in the grain-supported facies F5 (Figure 4h). The subordinate grains in facies F5 include bioclasts of bivalves (5%), echinoderms (10%) and brachiopods (25%). The bioclasts range in size from 1 mm to 1 cm. Well-preserved fossil specimens of marine benthic invertebrates (mainly brachiopods) with low diversity were observed in the outcrops of facies F5.

4.2.6. FACIES F6: BIOCLASTIC-INTRACLASTIC PACKSTONE/GRAINSTONE

Microscopic analyses indicate that the main components of this grain-supported facies include bioclasts of marine benthic invertebrates and carbonate intraclasts which are densely packed and embedded in a packstone to grainstone texture with a dominant microsparitic/sparitic groundmass (Figure 5a). The carbonate intraclasts are the dominant grains (60% of the grains) in facies F6. They are commonly micritized and subrounded and are approximately 3 mm to 1 cm in size. The bioclasts (35% of the grains) mainly include fragments of brachiopods and range in size from 8 mm to 5 cm. Very rare peloids (5% of the grains) are scattered in facies F6.

4.2.7. FACIES F7: CORAL-STROMATOPOROID BOUNDSTONE WITH INTERCALATIONS OF CORAL FLOATSTONE

Facies F7 is defined by the dominance and abundance of stromatoporoids, colonial hexagonarid rugose corals and solitary rugose corals

http://dx.doi.org/10.18268/BSGM2025v77n2a060625

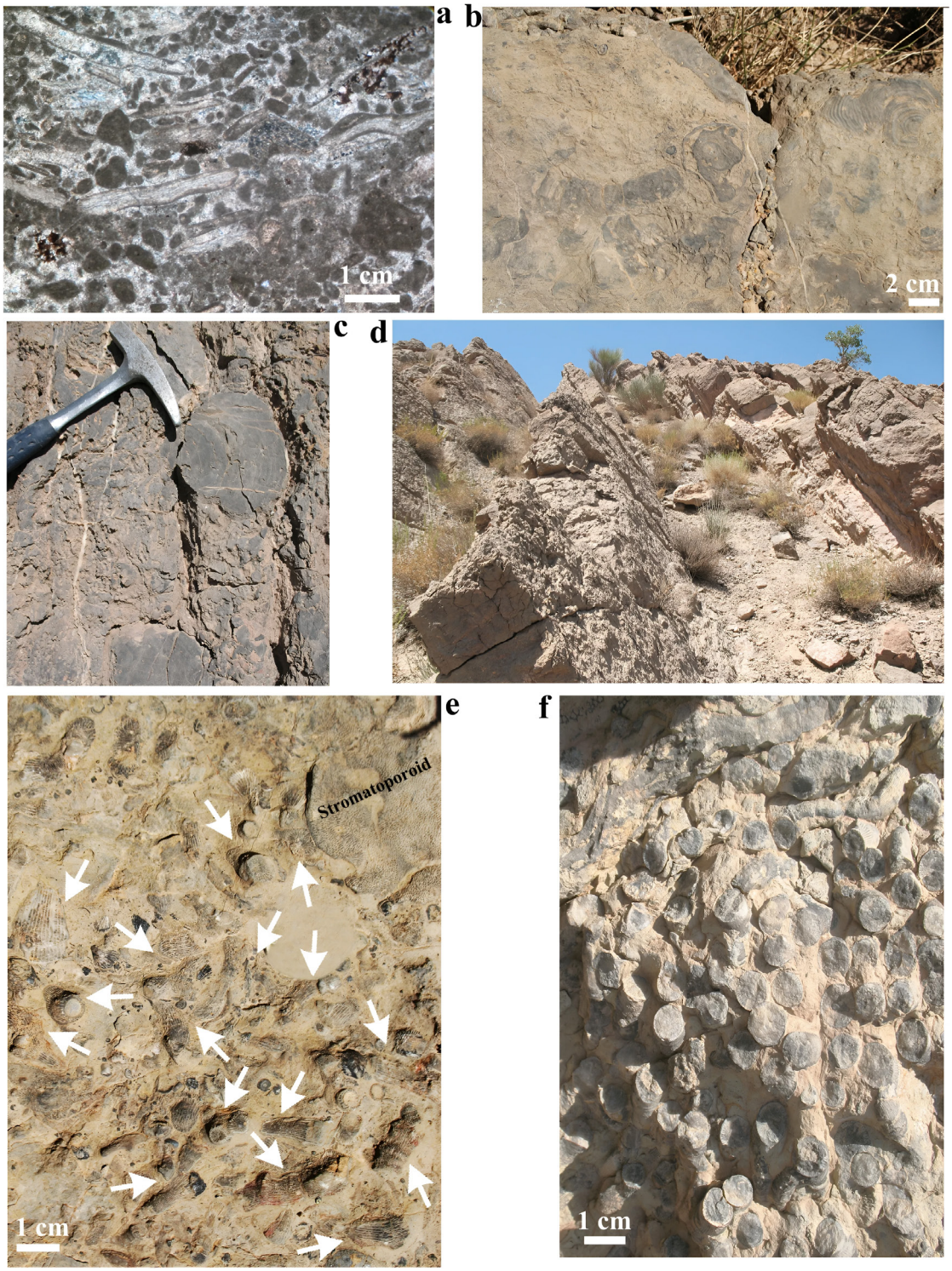

Figure 5 The identified facies in the studied succession of the Middle-Upper Devonian Bahram Formation, a) Thin-section microphotograph of bioclastic-intraclastic packstone/grainstone (F6). The carbonate intraclasts in the facies are commonly micritized, b–f) Fossils and outcrop views from facies F7 in the 70m-thick interval of biostromal limestone, b) Stromatoporoids with laminar growth form in the boundstone texture of facies F7, c) A domed-shaped stromatoporoid in the boundstone texture of facies F7, d) Outcrop view of facies F7 in the 70m-thick interval of biostromal limestone, e, f) Solitary rugose corals in the floatstone texture (representing coral floatstone facies) of facies F7. A micrite groundmass fills the space among the corals, e) The white arrows point to the solitary rugose corals. Solitary rugose corals occasionally co-occur with stromatoporoids and bryozoans.

http://dx.doi.org/10.18268/BSGM2025v77n2a060625

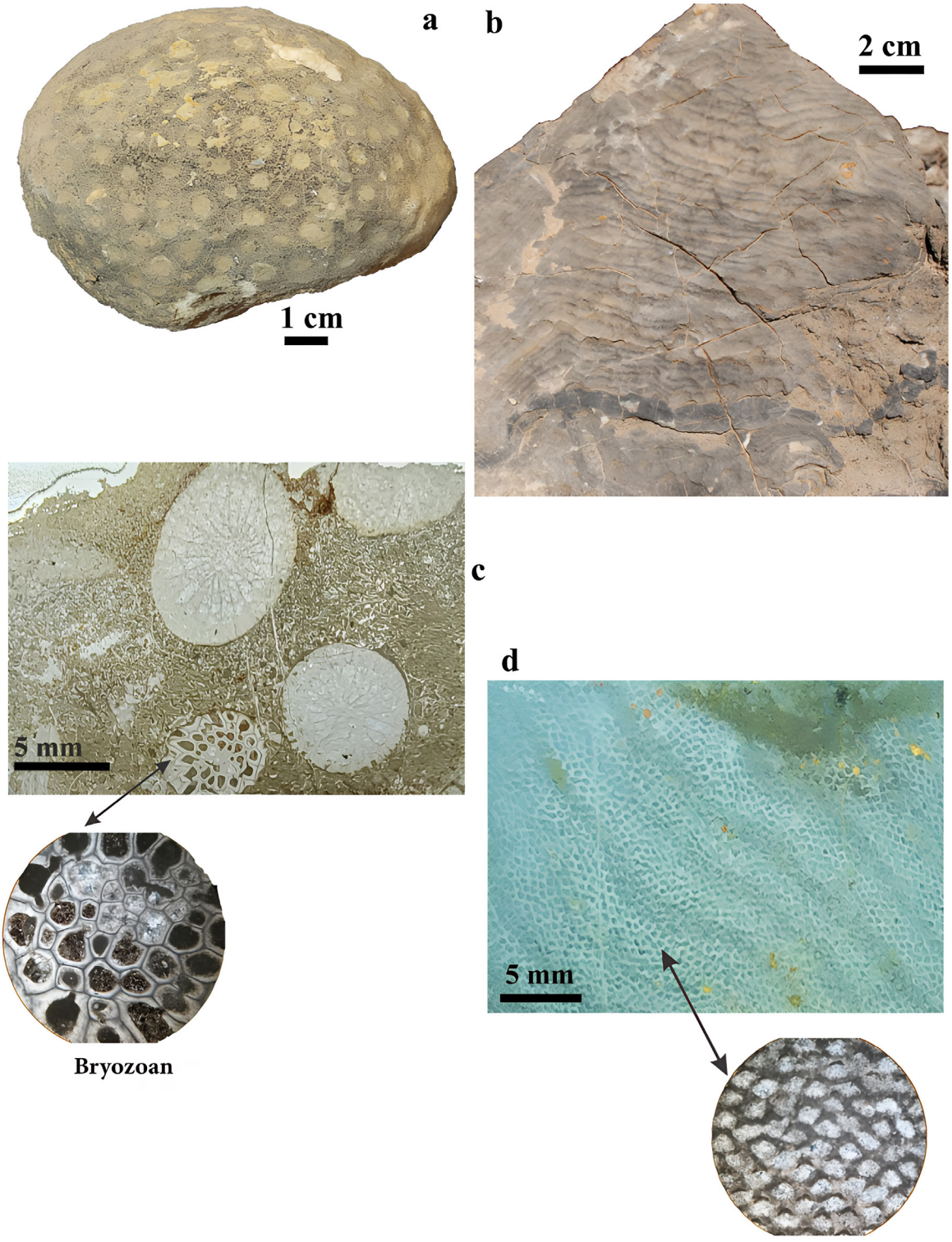

Figure 6 a) Field photo of a colonial hexagonarid rugose coral showing a cerioid massive growth form in the boundstone texture of facies F7, b) Field photo of a stromatoporoid with a laminar growth form in the boundstone texture of facies F7, c) Thin-section microphotograph of solitary rugose corals in the floatstone texture of facies F7 with a micritic groundmass (coral floatstone facies). A bryozoan is marked with an arrow on the microphotograph, d) Thin-section microphotograph of a stromatoporoid with a laminar growth form in facies F7.

http://dx.doi.org/10.18268/BSGM2025v77n2a060625

in the 70 m-thick interval of biostromal limestone in Unit B of the Bahram Formation (Figures 2, 5b, 5c, 5e, 5f and 6a-6d). Generally, the associations of the corals and stromatoporoids together form a rigid carbonate framework in the thick interval of biostromal limestone. Facies F7 is dominated by a boundstone texture. There are intercalations of floatstone texture (representing coral floatstone facies; Figures 5e, 5f and 6c) in facies F7. The boundstone texture of facies F7 is occupied and dominated by colonial hexagonaridrugose corals showing cerioid massive growth form and stromatoporoids displaying both laminar and dome-shaped growth forms (Figures 5b, 5c, 6a and 6b) co-occurred with subordinate biota such as bryozoans, brachiopods, and echinoderms and their fragments. The diameter of individual corals in a colony ranges from 6 mm to 1 cm (Figure 6a). The space or cavity within a number of individual corals is filled with calcite cement. The colonial hexagonarid rugose corals and stromatoporoids are commonly in situ and autochthonous. Reworked and allochthonous specimens of these benthic invertebrates are also present in the boundstone texture of facies F7, but are often intact. However, fragments of stromatoporoids also occur. The intercalations of floatstone texture in facies F7 in the biostromal limestone-bearing interval are composed of a micritic groundmass and are predominated by solitary rugose corals and represent coral floatstone facies (Figures 5e, 5f and 6c). A number of the solitary corals are autochthonous and in situ which are observable in the exposed deposits, whereas others are reworked; allochthonous and not in growth position but are commonly intact. Nevertheless, fragments of solitary corals, stromatoporoids and bryozoans are also present in the floatstone texture. The diameter of each solitary rugose coral ranges from 5 mm to 1 cm (Figures 5e, 5f and 6c). Micrite fills the space among the solitary rugose corals in the floatstone texture of facies 7 (Figures 5e, 5f and 6c). The solitary corals occasionally co-occur with stromatoporoids with laminar growth form and bryozoans (Figures 5e and 6c).

4.2.8. FACIES F8: BIOCLASTIC PACKSTONE

Microscopic studies show that this grain-supported facies contains abundant bioclasts of marine benthic invertebrates embedded in a packstone texture with a dominant microsparitic/sparitic groundmass (Figure 7a). The bioclasts are densely packed and include fragments of echinoderms (50%), brachiopods (45%) and bivalves (5%). The bioclasts are commonly 1 mm to5 mm in size, and a number of them are encrusted by micritic envelopes (Figure 7a).

4.2.9 FACIES F9: PELOIDAL-BIOCLASTIC-ONCOIDAL PACKSTONE/ GRAINSTONE

Stratigraphically, this oncoid-bearing facies (Figures 7b-7f) is deposited near the 70 m-thick interval of biostromal limestone (with boundstone facies intercalated with coral floatstone) in the studied succession of the Bahram Formation (Figure 2). Microscopic analyses indicate that this grain-supported facies is composed of a groundmass dominated by micrite (70% of the groundmass). The groundmass subordinately consists of sparite (30% of the groundmass). Oncoids (50% of the allochems), bioclasts of marine benthic invertebrates (30% of the allochems) and peloids (20% of the allochems) are densely packed in the groundmass. The bioclasts mainly (80%) include large fragments of bryozoans and stromatoporoids (Figures 7c, 7d and 7f) and subordinately comprise other bioclasts (20%). The bioclasts range in size from 0.2 mm to 8 mm. The peloids are 0.1 mm to 0.5 mm in diameter. The oncoids are 3 mm to 2 cm in size and are elongated, spherical and subspherical in shape. Some of the spherical/subspherical oncoids lack nucleus and are defined as full-cortex oncoids. However, all the elongated oncoids have nucleus. The nucleus in the oncoids mainly comprises fragments of bryozoans and other bioclasts (Figures 7d and 7e).

http://dx.doi.org/10.18268/BSGM2025v77n2a060625

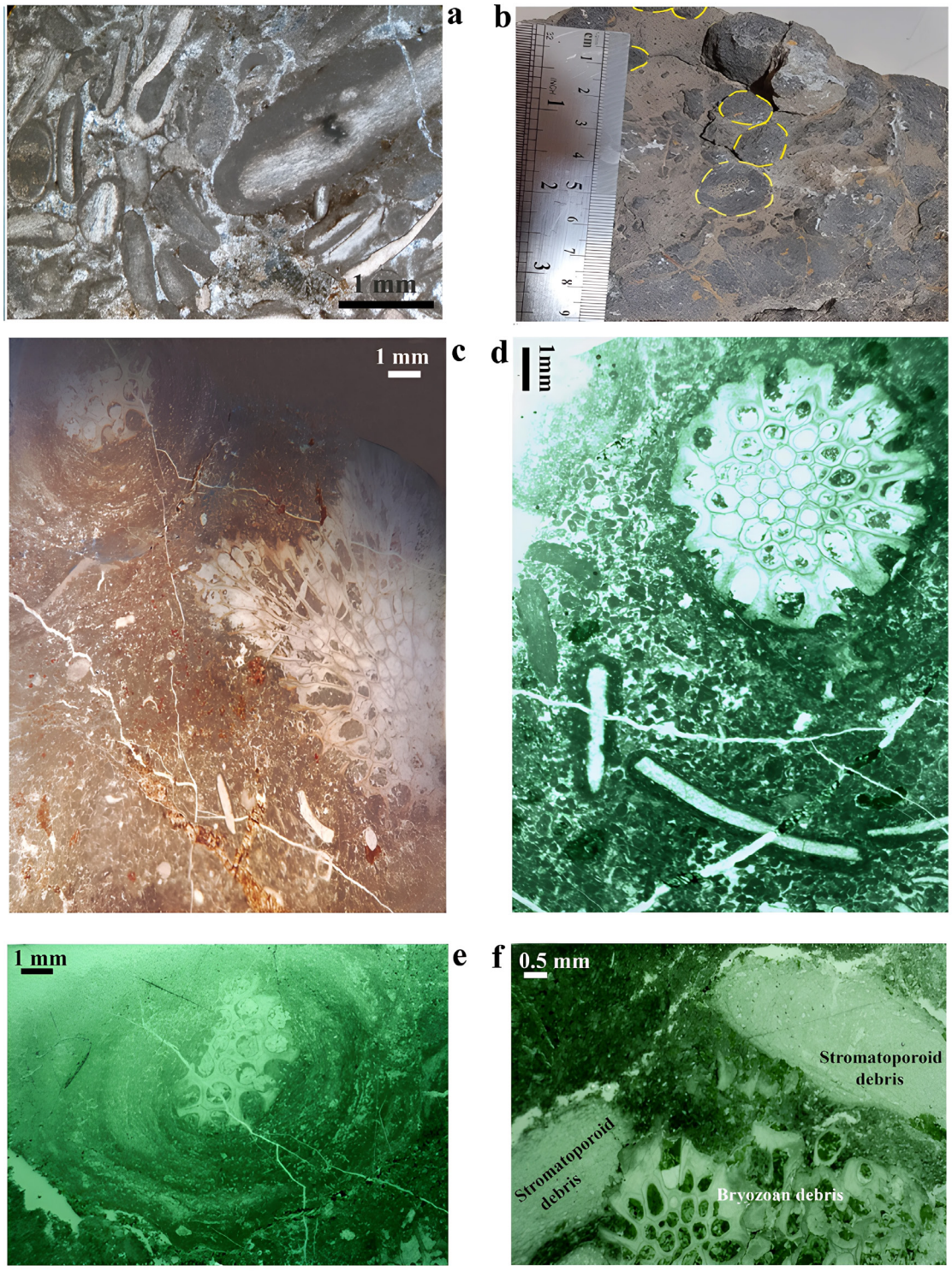

Figure 7 The identified facies in the studied succession of the Middle-Upper Devonian Bahram Formation, a) Bioclastic packstone (F8). A number of bioclasts in the facies are encrusted by micritic envelopes, b–f) Peloidal-bioclastic-oncoidal packstone/grainstone (F9), c) Micritic groundmass, scattered bioclasts, peloids, a large fragment of a bryozoan and an oncoid in facies F9, d) Sparitic groundmass, peloids, three elongated oncoids with nucleus and a large fragment of a bryozoan in facies F9. The fragment of bryozoan was used as a nucleus during the formation of a spherical oncoid that has not been completely formed. The nucleus of the elongated oncoids includes bioclasts, e) A subspherical oncoid with a nucleus in facies F9. The nucleus comprises a fragment of bryozoan, f) Fragments of bryozoans and stromatoporoids in facies F9, a, c, d, e and f: thin-section microphotographs, b): field photo.

http://dx.doi.org/10.18268/BSGM2025v77n2a060625

5. Interpretation

5.1. PALEOENVIRONMENTS

Generally, the type, diversity and stratigraphic position of facies are directly associated with different depositional conditions and changes in sedimentary paleoenvironments and therefore are useful tools in paleoenvironmental reconstructions (Einsele, 2000; Catuneanu, 2006; Flügel, 2010; Nichols, 2023). In this study, the stratigraphic and sedimentological features of the identified facies in the studied succession of the Bahram Formation (Figures 2 and 4-7) are indicative of tidal flat (including supratidal, intertidal and subtidal zones and tidal channels connecting to back-reef lagoon), back-reef lagoon and coral-stromatoporoid marginal reef (including reef crest and reef front zones) paleoenvironments (Figure 8 and Table 1).

5.1.1. TIDAL FLAT

Facies F1, F2, F3, F6 and F8 are generally indicative of a tidal flat paleoenvironment (Figure 8 and Table 1). The horizontal and cross beddings in the studied sandstone-bearing intervals with quartzarenite facies (facies F2), the stratigraphic positions of the intervals in the studied succession (Figure 2) as well as the textural maturity of the quartzarenite facies represent a shallow zone ranging from supratidal to intertidal in a tidal flat paleoenvironment (Flügel, 2020; Hashmie *et al.*, 2016; Cuen-Romero *et al.*, 2022). Additionally, the abundance and occurrence of trace fossils of the ichnogenus Skolithos in the studied sandstone-bearing intervals with quartzarenite facies and the maturity of quartzarenite facies are evidence of high-energy condition and presence of suspension feeders in a shallow supratidal to intertidal zone of a marine tidal flat environment (Seilacher, 1964; Parcha and Pandey, 2011; Zand-Moghadam *et al.*, 2014; Hashmie *et al.*, 2016; Cuen-Romero *et al.*, 2022).

Generally, dolomitization of mudstones and micrites occur in tidal flats (particularly in supratidal and intertidal zones of tidal flats) during humid and warm and near-surface conditions (Gregg and Sibely, 1984; Gregg and Shelton, 1990; Warren, 2000; Lasemi *et al.*, 2008; Salehi *et al.*, 2020). The sedimentological features and the stratigraphic position of facies F3 in the studied succession and its vertical association with other facies (facies F1, F5, F6 and F8; Figure 2) are representative of a tidal flat paleoenvironment (Figure 8 and Table 1). Dominance of micritic and muddy groundmass and the absence of fossils, bioclasts and non-skeletal grains in parts of facies F3 (F3a: unfossiliferous mudstone) reflect low-energy conditions (Gregg and Shelton, 1990; Adachi *et al.*, 2004; Hoseinabadi *et al.*, 2016). The dolomitized mudstone texture of facies F3 (F3a) was deposited in a paleoenvironmental zone ranging from supratidal to intertidal (Figure 8 and Table 1). The lack of fossils, bioclasts and bioturbations in the dolomitized mudstone texture of facies F3 (F3a) is indicative of unfavorable conditions for living of organisms in the environment (Wilson, 1975; Flügel, 2010; Brasier *et al.*, 2011; Salehi *et al.*, 2020). Dominance of fine-grained dolomites in the mudstone texture of facies F3 (F3a) proposes that dolomitization occurred under near surface condition during early stages of diagenesis in the tidal flat environment (Lasemi *et al.*, 2012; Hoseinabadi *et al.*, 2016).

Furthermore, changes in chemical compounds of dolomitizing solutions could be the factor resulted in producing the zoning pattern in a number of dolomite crystals in facies F3 (Johnson *et al.*, 2009; Hoseinabadi *et al.*, 2016). The scattered detrital quartz grains in the unfossiliferous mudstone texture (F3a) of facies F3 point to deposition in an environment near the land. The dolomitic wackestone texture of facies F3 (F3b) with reworked and scattered bioclasts of shallow marine benthic invertebrates is representative of the subtidal zone of the tidal flat paleoenvironment (Figure 8 and Table 1). Dolomitization of the wackestone texture occurred during diagenesis. Facies F1 (shale) can be assigned to a subtidal zone of the tidal flat paleoenvironment (Figure 8

http://dx.doi.org/10.18268/BSGM2025v77n2a060625

and Table 1) based on its sedimentary grains, its stratigraphic position and its vertical association with other facies in the studied succession (facies F2, F3, and F8; Figure 2).

The intercalation of shale (facies F1) with sandstone (facies F2) in the middle part of the studied succession of the Bahram Formation (Figure 2) is evidence of a mixed sand-mud tidal flat (Reineck and Singh, 1975; Hashmie *et al.*, 2016). The presence of fine-grained detrital quartz crystals and bioclasts of shallow marine benthic invertebrates in the shales of facies F1 reflects normal marine conditions in the tidal flat paleoenvironment (Warren, 2006) near the land. The dominance of microsparite/sparite, lack of micrite, accumulation of large and subrounded carbonate intraclasts and bioclasts of marine benthic invertebrates such as brachiopods in facies

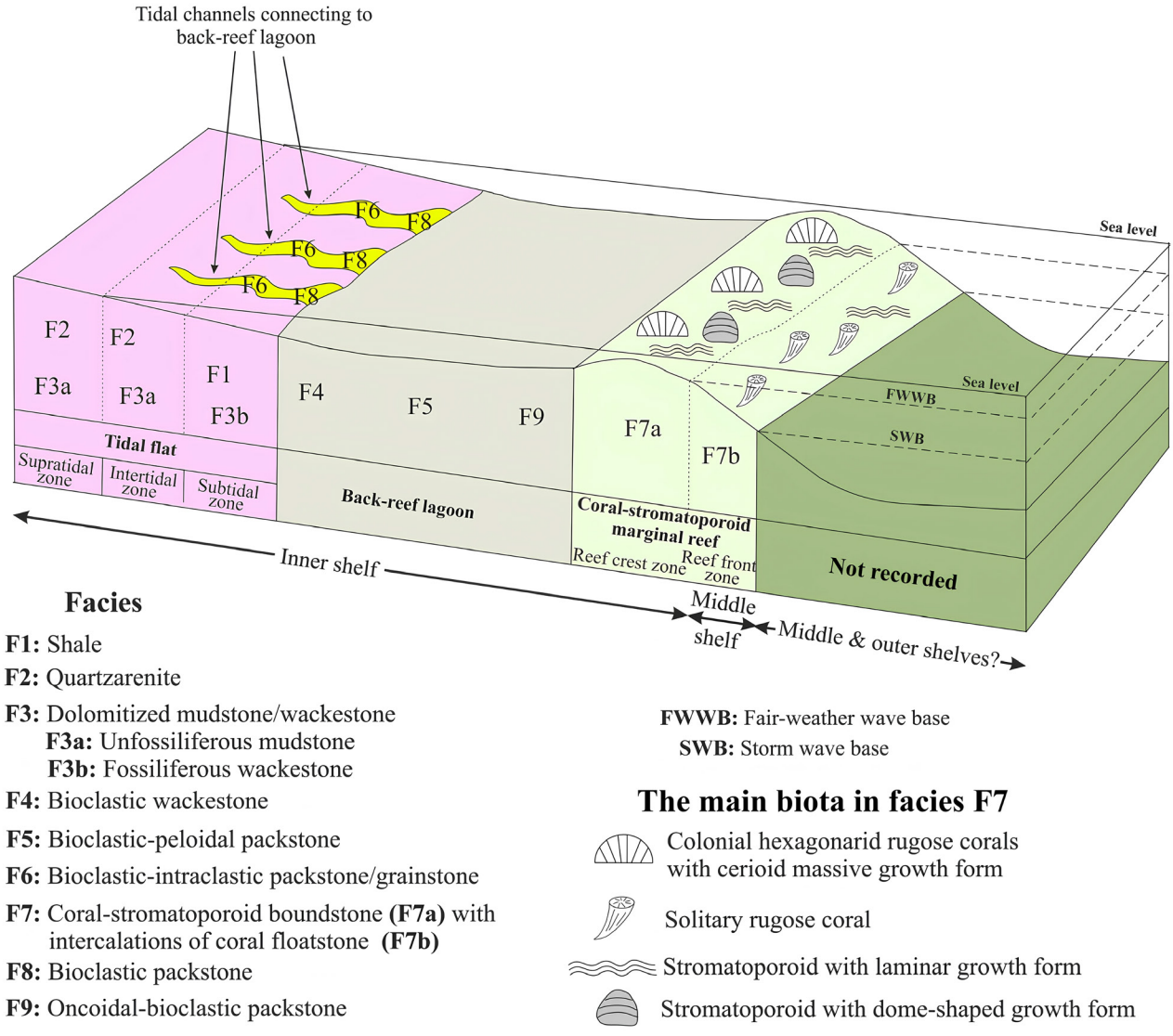

Figure 8 Paleoenvironments and depositional model of the Givetian–Famennian Bahram Formation in the studied succession. The depositional model of the formation is consistent with a mixed carbonate-clastic shallow marine rimmed shelf. Tidal flat and back-reef lagoon paleoenvironments as well as the reef crest zone of a coral-stromatoporoid marginal reef paleoenvironment were developed on an inner shelf, whereas the reef front zone of the marginal reef paleoenvironment was established on a middle shelf.

http://dx.doi.org/10.18268/BSGM2025v77n2a060625

F6 reflect high-energy tidal channels (Shinn, 1983, 1986; Flügel, 2010; Hoseinabadi *et al.*, 2016). The sedimentary features of facies F8 can also represent the same tidal channels. Generally, the sedimentary features and the stratigraphic position of facies F6 and F8 in the studied succession and their vertical associations with other facies (Figure 2) indicate that the tidal channels were in the tidal flat paleoenvironment (Figure 8 and Table 1).

The distribution of bioclasts encrusted by micritic envelopes, micritized carbonate intraclasts, very rare peloids and fragments of brachiopod and echinoderm in the microsparitic/sparitic groundmass of facies F8 and F6 suggests reworking and transportation of sedimentary grains from a lagoon paleoenvironment to the tidal flat paleoenvironment by the wave currents of the tidal channels. The high-energy conditions in the tidal channels resulted in removal of micrite and precipitation of sparry calcite cement or microsparite/sparite (Carozzi, 1989; Tucker and Wright, 1990) in the tidal flat paleoenvironment. However, the tidal channels were possibly passing through the subtidal and intertidal zones of the tidal flat paleoenvironment (Figure 8).

5.1.2. BACK-REEF LAGOON

Generally, the distribution of skeletal grains/allochems such as brachiopods, ostracods, bivalves, calcareous algae as well as none-skeletal grains/allochems such as peloids and oncoids in a micritic groundmass in facies F4, F5 and F9 (Table 1) points to a lagoon paleoenvironment above the fair-weather wave base (FWWB; Figure 8). The rareness of bioclasts, low diversity of fauna and the presence of peloids in facies F4 and its wackestone texture are evidence of low-energy conditions, quiet waters and the shoreward part of the lagoon restricted from an open marine (Wilson, 1975; Hine, 1977; Tamasovych, 2004; Hoseinabadi *et al.*, 2016; Salehi *et al.*, 2020; Nichols, 2023). The co-occurrence of bioclasts of brachiopods, ostracods, bivalves and calcareous algae in the micritic groundmass of facies F4 suggests a low-energy environment (Bachmann and Hirsch, 2006; Husince and Sokac, 2006; Hashmie *et al.*, 2016).

The presence of detrital quartz grains in facies F4 indicates that this facies was deposited near the land. Facies F4 represents parts of the lagoon near the tidal flat paleoenvironment (Figure 8). Dominance of peloids and the occurrence of bioclasts and some well-preserved fossil specimens of marine benthic invertebrates (mainly brachiopods) with low diversity in the packstone texture of facies F5 with a micritic groundmass propose that the facies was deposited in a low-energy shallow lagoon which was restricted from an open marine (Wilson, 1975; Hine, 1977; Tamasovych, 2004; Salehi *et al.*, 2020; Nichols, 2023). The occurrence of oncoids, peloids and micrite in facies F9 points to a lagoon paleoenvironment (Figure 8).

However, the stratigraphic position of facies F9 and its association with the 70 m-thick interval of biostromal limestone (with a coral-stromatoporoid boundstone facies intercalated with coral floatstone) in the Bahram Formation (Figure 2) as well as the presence of a subordinate sparitic groundmass and bioclasts dominated by large fragments of bryozoans and stromatoporoids in facies F9 indicate parts of the lagoon paleoenvironment close to a barrier or reefal environment (marginal reef in this study; Figure 8) and higher-energy conditions. Based on the identified lagoon facies and the other facies and the types of the reconstructed paleoenvironments in this study, the lagoon paleoenvironment can be considered as a back-reef lagoon (Figure 8).

5.1.3. CORAL-STROMATOPOROID MARGINAL REEF

The stratigraphy and lateral extension of the studied thick biostromal limestone-bearing interval composed of dominant boundstone texture intercalated with floatstone texture (facies F7) and the presence of a rigid carbonate framework and in situ and autochthonous corals and stromatoporoids in the biostromal

limestone-bearing interval propose a coral-stromatoporoid marginal reef paleoenvironment (Figure 8 and Table 1) that could form a barrier. An organic reef is proposed by the dominance of benthic in situ and autochthonous frame builders (Wilson, 1975; Wendt *et al.*, 2002; Flügel, 2010; Hashmie *et al.*, 2016) in the boundstone texture of facies F7 in the biostromal limestone-bearing interval.

In general, the marginal reef paleoenvironment exists as a rigid carbonate framework resistant to wave currents and is divided into reef crest (shallow) and reef front (deeper) zones (Figure 8 and Table 1). In this study, the back-reef zone overlaps with the lagoon paleoenvironment (back-reef lagoon). The reef crest zone above the fair-weather wave base (FWWB) is represented by the boundstone texture of facies 7 and was occupied by massive colonial rugose corals and laminar and dome-shaped stromatoporoids co-occurred with bryozoans, brachiopods, and echinoderms. In the reef crest zone, calcite cement filled the space in a number of individual corals in the colonies. The massive colonial rugose corals together with the dome-shaped stromatoporoids inhabited shallow waters and represent high sedimentation rates (Isaacson and Curran, 1981; Pohler, 1998; Pellegrini *et al.*, 2012).

However, the stromatoporoids with laminar growth form indicate periods with lower sedimentation rates and normal water turbulence (Königshof and Kershaw, 2006). The massive colonial corals indicate the prevalence of a suitable hard substrate for colonization of benthic organisms (Brett, 1988; Hashmie *et al.*, 2016) and shallow and high water energy (Fernández-Martínez *et al.*, 2010) in the reef crest zone. High water energy and possibly storm or wave currents periodically resulted in reworking of a number of massive colonial corals and stromatoporoids (Corlett and Jones, 2011; Da Silva *et al.*, 2011; Hashmie *et al.*, 2016) and fragmentation of stromatoporoids, bryozoans, echinoderms, and brachiopods. The reef front zone below the fair-weather wave base (FWWB) and above the storm wave base (SWB) and in the deeper parts of the marginal reef paleoenvironment is indicated by the floatstone texture of facies F7 and was predominantly populated by solitary corals (MacNeil and Jones, 2016) co-occurred with rare stromatoporoids with laminar growth form (Figure 8) and bryozoans. Deposition of the micritic groundmass in the floatstone texture and among the solitary corals suggests low water energy (Hashmie *et al.*, 2016) in the reef front zone.

The presence of stromatoporoids in a micritic groundmass reflects normal water turbulence and low sedimentation rates (Königshof and Kershaw, 2006; Corlett and Jones, 2011; Pellegrini *et al.*, 2012). In general, the floatstone texture of facies F7 formed when the growth rate of the reef decreased and the quiet environmental conditions prevailed and resulted in deposition of micrite or mud (Corlett and Jones, 2011). However, high-energy events periodically interrupted low sedimentation rate (Corlett and Jones, 2011) and led to reworking and fragmentation of a number of solitary corals, stromatoporoids and bryozoans in the reef front zone.

6. Discussion

6.1. DEPOSITIONAL MODEL OF THE BAHRAM FORMATION IN THE STUDIED AREA

The stratigraphy, facies types and the reconstructed paleoenvironments of the Bahram Formation in the studied succession, suggest a mixed carbonate-clastic shallow marine rimmed shelf during the Givetian–Famennian (Figure 8). The tidal flat and back-reef lagoon paleoenvironments as well as the reef crest zone of the coral-stromatoporoid marginal reef paleoenvironment were developed on the inner zone of the shelf (inner shelf), whereas the reef front zone of the reef paleoenvironment was established on the middle zone of the shelf (middle shelf), see Figure 8. Generally, shallow marine mixed carbonate-clastic shelves can be suggested by the presence and co-occurrence of

http://dx.doi.org/10.18268/BSGM2025v77n2a060625

carbonate grains such as algae, peloids, oncoids, abundant carbonate intraclasts and quartz grains in the environment as well as development of reefal facies, high-energy reefs/shoals and protected lagoons (Schlager, 2005; Flügel, 2010; Vaziri *et al.*, 2012; Hoseinabadi *et al.*, 2016; Hashmie *et al.*, 2016; Salehi *et al.*, 2020).

In general, reef environments are significantly more developed in rimmed platforms/shelves than in carbonate ramps (Einsele, 2000). Significant local clastic inputs from the land areas periodically led to deposition of the sandstone (quartzarenite) and shale facies in the tidal flat paleoenvironment in the inner zone (inner shelf) of the studied mixed carbonate-clastic shallow marine rimmed shelf (Figure 8) during the Givetian–Famennian. The margin of the studied mixed carbonate-clastic rimmed shelf was developing as a marginal reef paleoenvironment by colonization of corals and stromatoporoids (facies F7; Figures 2 and 8) during the lack of any important clastic inputs. Generally, during the Devonian, the paleogeography of the continents and extension of marine shelf paleoenvironments in the tropical regions contributed to development of shallow-water coral-stromatoporoid reefs that are representative of the most extensive reefs on the earth (Copper, 1994; Copper and Scotese, 2003; Corlett and Jones, 2011; Zapalski *et al.*, 2021).

The biotic communities in these reefs include: rugose corals, tabulate corals, stromatoporoids and colonies of bryozoans (Edinger *et al.*, 2002; Fagerstrom and Bradshaw, 2002; Pellegrini *et al.*, 2012; Zapalski *et al.*, 2021). However, the Devonian reefs developed and were common during the Givetian and Frasnian (Copper, 2002a; Copper and Scotese, 2003) but were drastically decreased around during the Frasnian-Famennian boundary (Copper, 2002b; Huang *et al.*, 2022).

6.2. DEPOSITION OF THE BAHRAM FORMATION IN THE IRAN PLATE

The Iran Plate was located in the southern margin of the Paleo-Tethys Ocean and north of the Gondwana at latitude near 30° S during the Devonian (Berberian and King, 1981; Scotese and McKerrow, 1990; Joachimski *et al.*, 2009; Scotese, 2014). In the Permian, the Iran Plate separated from the Gondwana and subsequently collided with the Turan Plate in the Eurasia in the Late Triassic during the closure of the Paleo-Tethys Ocean (Stöcklin, 1974; Wilmsen *et al.*, 2009).

During the Devonian, grabens and horsts and/or subsidence resulted in the deposition of ca 2000 m thick skeletal limestones, dolostones, shales and sandstones (Wendt *et al.*, 1997, 2002, 2005; Königshof *et al.*, 2017). In the Early and Middle Devonian, a long-term period of intertidal and nearshore conditions prevailed in the Iran Plate and the Padeha Formation was deposited (Wendt *et al.*, 2002; Hashmie *et al.*, 2016).

In the Middle-Late Devonian, a sea level rise led to flooding of a wide areas and development of mostly extended carbonate platforms, ramps, and shelves in the dominant shallow marine settings (Wendt *et al.*, 2002, 2005; Königshof *et al.*, 2017; Salehi *et al.*, 2020), and deposition of the Bahram Formation in northern margin of the Gondwana in a divergent and passive margin (Domeier and Torsvik, 2014; Hashmie *et al.*, 2016).

The Middle-Upper Devonian shales and sandstones in the Bahram Formation originated from local inputs of clastic sediments from erosion of the land and continental environments (Wendt *et al.*, 2002; Ghorbani, 2019; Zamani *et al.*, 2021). Although some fine-grained mudstone/shale intervals in the Bahram Formation were deposited in the low-energy parts of an open marine in an outer ramp below the storm wave base in the west of the Central-East Iranian Microcontinent (see Salehi *et al.*, 2020).

In the southeast of the town of Anarak in the Yazd Block (west of the Central-East Iranian Microcontinent), the Middle-Upper Devonian carbonate-dominated Bahram Formation was deposited on a homoclinal carbonate ramp (Figure 9) consisting of tidal flat, lagoon, shoal, and open marine paleoenvironments developed on the inner, middle and outer parts of the ramp during the absence of high-energy reefal frameworks (Salehi

et al., 2020). However, a local lagoonal biostrome formed by stromatoporoid bio-floatstone to rudstone facies comprising globular and dendroid stromatoporoids was established on the carbonate ramp (Salehi *et al.*, 2020). The deepest parts of the open marine paleoenvironment are indicated by the low-energy parts of the outer ramp (represented by fine-grained mudstone/laminated shale containing tentaculitids, crinoids and brachiopods) below the storm wave base (see Salehi *et al.*, 2020). Hoseinabadi *et al.* (2016) proposed that the strata of the Bahram Formation in the Tabas Block (in the Central-East Iranian Microcontinent) were deposited on a homoclinal carbonate ramp (Figure 9; comprising shore face, tidal flat, lagoonal, shoal and open-marine paleoenvironments) during the Middle-Late Devonian. The deepest parts of the open marine paleoenvironment are indicated by the lower energy parts (represented by bioclastic rudstone/floatstone facies containing brachiopods, bryozoans, echinoderms in a muddy groundmass) of the outer ramp below the fair-weather wave base (see Hoseinabadi *et al.*, 2016). In the northernmost part of the Tabas Block (south of the town of Kashmar; Figure 9), the carbonate ramp of the Bahram Formation consists of extended and the deepest open marine and limited tidal flat paleoenvironments and lacks the shore face paleoenvironment (see Hoseinabadi *et al.*, 2016). The carbonate ramp of the formation comprises shore face, more developed tidal flat and shoal paleoenvironments as well as limited and less developed open marine paleoenvironment in the northeast (south of Ozbak-kuh) and southeast of the town of Tabas in the more southern parts of the Tabas Block (see Hoseinabadi *et al.*, 2016). A shore face paleoenvironment represented by sublitharenite sandstone and a shoal paleoenvironment (in the middle ramp) partially comprising coral boundstone facies were developed in the southeast of the town of Tabas (Hoseinabadi *et al.*, 2016).

The researches carried out by Mahmoudi *et al.* (2015) showed that the Middle-Late Devonian carbonate deposits of the Bahram Formation in the east of Ozbak-kuh, north of the town of Tabas (in the Tabas Block) were accumulated on a ramp-type carbonate platform (possibly a homoclinal carbonate ramp; Figure 9). Inner ramp (including tidal flat and lagoon paleoenvironments), middle ramp (including shoal paleoenvironment and tidal channels) and outer ramp (including open marine paleoenvironment) were established on the platform (Mahmoudi *et al.*, 2015). The deepest parts of the open marine paleoenvironment are represented by the low-energy parts of the outer ramp below the fair-weather wave base and near or below the storm wave base (possibly near the basin; see Mahmoudi *et al.*, 2015). The low-energy parts of the outer ramp are represented by silty mudstone (dominated by sponge spicule and radiolarian molds) and peloidal wackestone (mainly containing peloids and subordinately containing sponge spicules) facies (see Mahmoudi *et al.*, 2015). Biostromal facies, corals and stromatoporoids were not reported from the carbonate platform.

Königshof *et al.* (2017) studied a mixed shallow-water carbonate-clastic succession of the Bahram Formation in the northeast of the city of Isfahan (Zefreh Section), between central Iran and the western part of the Central-East Iranian Microcontinent (Figure 9). They concluded that the Bahram Formation was deposited on a shallow homoclinal carbonate ramp (Figure 9) during the Givetian to Frasnian. The carbonate ramp was influenced by local clastic inputs from adjacent eroded lands (Königshof *et al.*, 2017). Tidal flat, lagoon, oolitic and bioclastic sandy shoal and shallow open marine paleoenvironments were established on the inner and middle parts of the ramp (see Königshof *et al.*, 2017). The deepest parts of the shallow open marine paleoenvironment are indicated by the low-energy and deepest parts of the middle ramp below the fair-weather wave base. The low-energy and deepest parts of the middle ramp are represented by organic-rich argillaceous lime mudstones and siltstones with rare bioturbations (Königshof *et al.*, 2017). A local biostrome and mini-mounds consisting of framestone and bafflestone facies

http://dx.doi.org/10.18268/BSGM2025v77n2a060625

with in situ stromatoporoids and coral colonies were developed on an environment ranging from the distal inner ramp to the middle ramp (possibly the shoal paleoenvironment in the inner ramp and middle ramp; Königshof *et al.*, 2017). However, the lithostratigraphic and facies details of the Bahram Formation in the Zefreh section (Königshof *et al.*, 2017) indicate that the depositional model of the formation can also be consistent with a mixed carbonate-clastic system (Figure 9).

Mixed carbonate-clastic shallow marine successions and depositional models of the Bahram Formation, biostromal limestones, reefal shoals/barriers/buildups and extended reefal frameworks and paleoenvironments were widely developed in the north of the Kerman area or the city of Kerman (Figure 9) in the south of the Tabas Block during the Middle and Late Devonian (*e.g.*, Wendt *et al.* 2002; Hashmie *et al.*, 2016; Hassani *et al.*, 2020 and this study). However, deeper open marine and near basin facies and paleoenvironments of the Bahram Formation are absent or very limited in the Kerman area.

Hassani *et al.* (2020) studied the Bahram Formation near the Sarashk village in the north of the city of Kerman and concluded that the Bahram Formation was established on a mixed carbonate-siliciclastic ramp during the Late

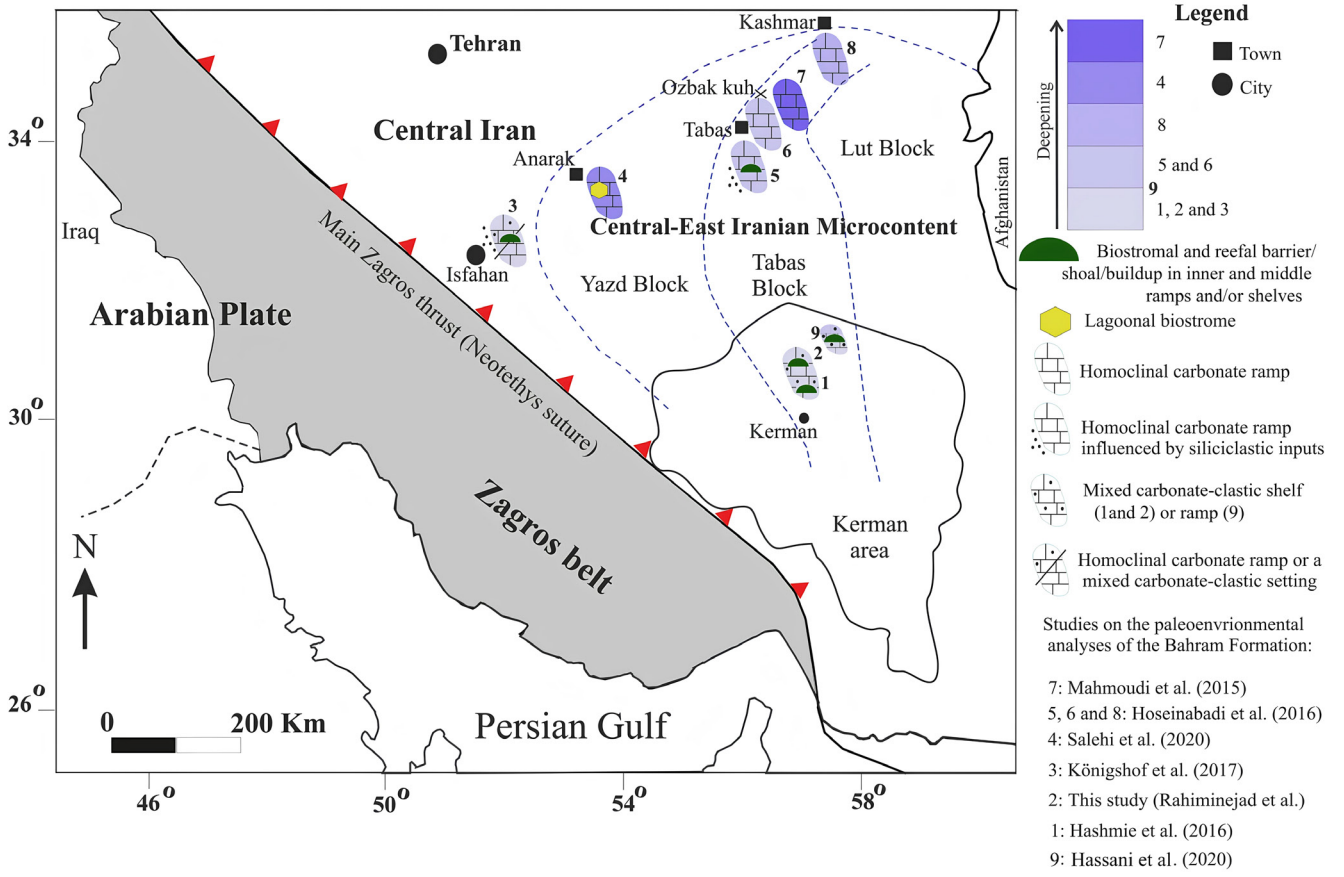

Figure 9 **Distribution map of the depositional models of the Middle-Upper Devonian Bahram Formation in the central Iran and the Central-East Iranian Microcontinent, based on previous studies and this study. (The map is modified and redrawn from Wilmsen et al., 2009; Rahiminejad and Zand-Moghadam, 2018). Details of the paleoenvironments of the depositional models are discussed in the text (the discussion chapter). From the northern parts of the Central-East Iranian Microcontinent towards its southern parts and the central Iran, the mixed carbonate-clastic shallow marine depositional systems of the Bahram Formation and the biostromal and reefal barriers/shoals/buildups and extended reefal frameworks and paleoenvironments associated with the inner and middle ramps and/or shelve settings of the formation were developed.**

Devonian (Figure 9). The ramp consists of an outer ramp, middle ramp, inner ramp, near-shore and supratidal zones (Hassani *et al.*, 2020). The deepest parts of the ramp are indicated by the outer ramp zone, reflected by crinoid echinoderm peloid wackestone and black organic-rich shale (containing shell debris and peloids) facies (see Hassani *et al.*, 2020). Coral buildups consisting of coral framestone (dominated by rugose corals) and bafflestone (comprises corals and sparse stromatoporoids) facies were developed on the middle parts of the mixed carbonate-siliciclastic ramp (see Hassani *et al.* 2020).

Additionally, coral-algal rudstone facies was deposited in the open inner ramp (see Hassani *et al.*, 2020). In the southwest of the Sarashk village (Hassani *et al.*, 2020; Figure 9), the Bahram Formation near the villages of Hutk and Sardar in the north of the city of Kerman was deposited on a mixed carbonate-siliciclastic shallow shelf (Hashmie *et al.*, 2016; Figure 9). Shallow open marine, high-energy shoal/barrier, lagoon, tidal flat, mud flat and shore paleoenvironments were established on the shelf (see Hashmie *et al.*, 2016). The deepest parts of the shallow open marine paleoenvironment and the shelf are represented by a bioclastic packstone/wackestone facies (containing bioclasts of bryozoans, echinoderms, brachiopods, bivalves, and gastropods) deposited under low-energy conditions below the storm wave base and below the seaward shoal/barrier (see Hashmie *et al.*, 2016). The high-energy shoal/barrier paleoenvironment on the mixed carbonate-siliciclastic shelf represents a patch reef consisting of a biostromal coral framestone facies dominated by rugose and tabulate corals with domal and massive colonies co-occurred with bryozoans (Hashmie *et al.*, 2016) in the inner shelf and possibly the middle shelf. Nevertheless, this laterally limited patch reef was influenced by periodic storms during the early stages of its development (see Hashmie *et al.*, 2016).

In the north of the Kerman area, the mixed carbonate-clastic depositional system of the Bahram Formation near the Sarashk village (see Hassani *et al.*, 2020) is slightly deeper than the mixed carbonate-clastic sedimentary models of the formation near the villages of Hutk and Sardar (Hashmie *et al.*, 2016) and the rimmed shelf system between the villages of Gerik and Shahzadeh Mohammad (this study; Figures 8 and 9). The depth trend between different localities is shown in Figure 9.

Generally, the mixed carbonate-clastic shallow marine rimmed shelf depositional model of the Bahram Formation developed between the villages of Gerik and Shahzadeh Mohammad (this study; Figures 1, 8, and 9), north of the villages of Hutk and Sardar represents the thickest biostromal framework and the most developed and widest lateral extension of reefal paleoenvironments during the Middle-Late Devonian of the north of the Kerman area. The extended marginal reef paleoenvironment on the rimmed shelf in this study was populated by more diverse frame builders dominated by stromatoporoids and both solitary and colonial corals co-occurred with bryozoans.

7. Conclusions

In the central Iran and the Central-East Iranian Microcontinent in the Iran Plate, the Middle-Upper Devonian Bahram Formation mainly was deposited on a homoclinal carbonate ramp. From the northern parts of the Microcontinent towards its southern parts and the central Iran, a decrease in water depth (a shallowing trend) and gradual increase in clastic inputs from the land areas resulted in development of mixed carbonate-clastic shallow marine depositional systems of the Bahram Formation.

Additionally, biostromal and reefal barriers/shoals associated with the inner and middle ramps and/or shelves of the Bahram Formations were developed towards the same shallowing-trend and direction in the Iran Plate. The Bahram Formation in the north of the Kerman area in the south of the Central-East Iranian Microcontinent

can represents one of the most extended mixed carbonate-clastic shallow marine sedimentary models during the Middle-Late Devonian of central and eastern Iran.

In this study, detailed facies and stratigraphic aspects of a 274 m thick mixed carbonate-clastic succession of the Bahram Formation were investigated in the north of the Kerman area, south of the Tabas Block in the south of the Central-East Iranian Microcontinent. The studies show that the formation consists of two clastic and seven carbonate facies deposited in tidal flat, back-reef lagoon and coral-stromatoporoid marginal reef paleoenvironments. The paleoenvironments were established on the inner and middle parts of a mixed carbonate-clastic shallow marine rimmed shelf during the Givetian-Famennian. This paper introduces a rare sedimentary model for the depositional system of the Middle-Upper Devonian Bahram Formation in the north of the Kerman area for the first time.

Contributions of authors

(1) conceptualization: AHR; (2) analysis or data acquisition: AHR, HB; (3) methodologic/technical development: AHR; (4) writing of the original manuscript: AHR; (5) writing of the corrected and edited manuscript: AHR; (6) graphic design: AHR; (7) fieldwork: AHR; HB; (8) interpretation: AHR; (9) financing: AHR, HB; (10) data preparation: HB.

Financing

This study was done without financial support.

Acknowledgements

The authors gratefully acknowledge the Editor-in-Chief for the editorial handling and the reviewers for their valuable and useful suggestions and comments that contributed to improvement of the manuscript.

Dr. Hamed Zand-Moghadam (Shahid Bahonar University of Kerman) and Dr. Hamed Ameri (Graduate University of Advanced Technology, Kerman) are greatly appreciated for their helpful contributions during the fieldwork.

Conflicts of interest

The authors declare that there are no conflicts of interest.

Handling editor

Francisco J. Vega

References

Adachi, N., Ezaki, Y., Liu, J., 2004, The origins of peloids immediately after the end Permian extinction, Guizhou Province, South China: Sedimentary Geology, 164, 161–178. https://doi.org/10.1016/j.sedgeo.2003.10.007

Aghanabati, A., 2004, Geology of Iran: Tehran, Iran, Geological Survey of Iran, 586 p.

Ahmadi, T., Dastanpour, M., Vaziri, M.R., 2012, Upper Frasnian (Upper Devonian) polygnathus and icriodus conodonts from the Bahram Formation, Hur section, Kerman province, Southeastern Iran: Rivista Italiana di Paleontologia e Stratigrafia, 118(2), 203–212. https://doi.org/10.13130/2039-4942/6000

Bachmann, M., Hirsch, F., 2006, Lower Cretaceous carbonate platform of the eastern Levant (Galilee and the Golan Heights): stratigraphy and second-order sea-level change: Cretaceous Research, 27, 487–512. https://doi.org/10.1016/j.cretres.2005.09.003

Bahrami, A., Königshof, P., Boncheva, I., Tabatabaei, M.S., Yazdi, M., Safari, Z., 2015, Middle Devonian (Givetian) conodonts from the northern margin of Gondwana (Soh and Natanz regions, north-west Isfahan, Central Iran): biostratigraphy and palaeoenvironmental implications: Palaeobiodiversity and Palaeoenvironments,

95, 555–577. https://doi.org/10.1007/s12549-015-0205-0

Bahrami, A., Zamani, F., Corradini, C., Yazdi, M., Ameri, H., 2014, Late Devonian (Frasnian) conodonts from the Bahram Formation in the Sar-eAshk Section, Kerman province, Central-East Iran Microplate: Bollettino della Società Paleontologica Italiana, 53(3),179–188.

Berberian, M., King, G.C.P., 1981, Towards a palaeogeography and tectonic evolution of Iran: Canadian Journal of Earth Sciences, 18, 210–265. https://doi.org/10.1139/e81-019

Brasier, A.T., Fallick, A.E., Prave, A.R., Melezhik, A.V., Lepland, A., 2011, Coastal sabkha dolomites and calcitised sulphates preserving the Lomagundi-Jatuli carbon isotope signal. Precambrian Research, 189(1–2), 193–211. https://doi.org/10.1016/j.precamres.2011.05.011

Brett, C.E., 1988, Paleoecology and evolution of marine hard substrate communities: an overview: Palaios, 3(4), 374–378. https://doi.org/10.2307/3514783

Carozzi, A.V., 1989, Carbonate rock depositional model: a microfacies approach: USA, Prentice-Hall, 604 p.

Catuneanu, O., 2006, Principles of Sequence Stratigraphy: Amsterdam, Boston, Heidelberg, London, New York, Elsevier, 375 p.

Chiarella, D., Longhitano, S.G., 2012, Distinguishing depositional environments in shallow- water mixed, bio-siliciclastic deposits on the basis of the degree of heterolithic segregation (Gelasian, southern Italy): Journal of Sedimentary Research, 82, 969–990. https://doi.org/10.2110/jsr.2012.78

Chiarella, D., Longhitano, S.G., Sabato, L., Tropeano, M., 2012, Sedimentology and hydrodynamics of mixed (siliciclastic-bioclastic) shallow-marine deposits of Acerenza (Pliocene, Southern Apennines, Italy): Italian Journal of Geosciences, 131, 136–151. https://doi.org/10.3301/IJG.2011.36

Copper, P., 1994, Ancient reef ecosystem expansion and collapse: Coral Reefs, 13(1), 3–11. https://doi.org/10.1007/BF00426428

Copper, P., 2002a, Silurian and Devonian reefs: 80 million years of global greenhouse between two ice ages, in Kiessling, W., Flügel, E., Golonka, J. (eds.), Phanerozoic Reef Patterns: Tulsa, Oklahoma, SEPM Special Publication No. 72, 181–238.

Copper, P., 2002b, Reef development at the Frasnian/Famennian mass extinction boundary: Palaeogeography, Palaeoclimatology, Palaeoecology, 181, 27–65. https://doi.org/10.1016/S0031-0182(01)00472-2

Copper, P., Scotese, C.R., 2003, Megareefs in Middle Devonian supergreenhouse climates: Geological Society of America Special Paper, 370, 209–230. https://doi.org/10.1130/0-8137-2370-1.209

Corlett, H., Jones, B., 2011, Ecological controls on Devonian stromatoporoid-dominated and coral-dominated reef growth in the Mackenzie Basin, Northwest Territories, Canada: Canadian Journal of Earth Sciences, 48(12), 1543–1560. https://doi.org/10.1139/e11-056

Cuen-Romero, F.J., Montijo-González, A., Monreal, R., Sundberg, F.A., Espinoza-Maldonado, G., Grijalva-Noriega, F.J., Noriega-Ruiz, H.A., Minjárez-Sosa, I., Ochoa-Granillo, J.A., 2022, Cambrian (Series 2 to Miaolingian) platform facies from central Sonora, Mexico and the regional correlation: Palaeoworld, 31(1), 41–57. https://doi.org/10.1016/j.palwor.2021.03.002

Da Silva, A.C., Kershaw, S., Boulvain, F., 2011, Stromatoporoid palaeoecology in the Frasnian (Upper Devonian) Belgian platform, and its applications in interpretation of carbonate platform environments: Palaeontology, 54(4), 883–905. https://doi.org/10.1111/j.1475-4983.2011.01037.x

http://dx.doi.org/10.18268/BSGM2025v77n2a060625

Dickson, J.A.D., 1966, Carbonate identification and genesis as revealed by staining: Journal of Sedimentary Research, 36, 441–505. https://doi.org/10.1306/74D714F6-2B21-11D7-8648000102C1865D

Domeier, M., Torsvik, T.H., 2014, Plate tectonics in the late Paleozoic: Geoscience Frontiers, 5, 303–350. https://doi.org/10.1016/j.gsf.2014.01.002

Dunham, R.J., 1962, Classification of carbonate rocks according to depositional textures, in Ham, W.E. (ed.), Classification of carbonate rocks: U.S.A., AAPG, Memoir, 1,108–121.

Edinger, E.N., Copper, St.P., Risk, M.J., Atmojo, W., 2002, Oceanography and reefs of recent and Paleozoic tropical epeiric seas: Facies, 47, 127–149. https://doi.org/10.1007/BF02667710

Einsele, G., 2000, Sedimentary basins: Evolution, Facies, and Sediment Budget: Berlin, Heidelberg, Springer, 792 p. https://doi.org/10.1007/978-3-662-04029-4

Embry, A.F., Klovan, J.E., 1971, A late Devonian reef tract on Northeastern Banks Island, NWT: Bulletin of Canadian Petroleum Geology, 19, 730–781. https://doi.org/10.35767/gscpgbull.19.4.730

Fagerstrom, J.A., Bradshaw, M.A., 2002, Early Devonian reefs at Reefton, New Zealand: guilds, origin and paleogeographic significance: Lethaia, 35, 35–50. https://doi.org/10.1111/j.1502-3931.2002.tb00066.x

Fernández-Martínez, E., Fernández, L.P., Méndez-Bedia, I., Soto, F., Mistiaen, B., 2010, Earliest Pragian (Early Devonian) corals and stromatoporoids from reefal settings in the Cantabrian Zone (N Spain): Geologica Acta, 8(3), 301–323. https://raco.cat/index.php/GeologicaActa/article/view/202808

Ferronatto, J.P.F., dos Santos Scherer, C.M., Drago, G.B., Rodrigues, A.G., de Souza, *E.g.*, dos Reis, A.D., Bállico, M.B., Kifumbi, C., Cazarin, C.L., 2021, Mixed carbonate-siliciclastic sedimentation in a Mesoproterozoic storm-dominated ramp: Depositional processes and stromatolite development: Precambrian Research, 361, 106240. https://doi.org/10.1016/j.precamres.2021.106240

Flügel, E., 2010, Microfacies of carbonate rocks, analysis interpretation and application: Berlin, Springer, 984 p. https://doi.org/10.1007/978-3-642-03796-2

Folk, R.L., 1980, Petrology of Sedimentary Rocks: Austin, Hemphill Publishing Company, 184 p.

Gholamalian, H., 2006, Biostratigraphy of Late Devonian Sequence in Hutk section (North of Kerman) Based on Conodonts (in Farsi, abstract in English): Geosciences Scientific Quarterly Journal (Ulum-I Zamin), 15(59), 94–101.

Gholamalian, H., Sajadi, S.H., Hassani, M.J., 2015, Biostratigraphy of Devonian succession (Bahram Formation) in Sardar section, North of Kerman based on conodonts (in Farsi, abstract in English): Paleontology, 2(2), 198–211.

Ghorbani, M., 2019, Lithostratigraphy of Iran: Dordrecht, Springer, 274 p.

Gregg, J.M., Shelton, K.L., 1990, Dolomitization and dolomite neomorphism in the back reef facies of the Bonneterre and Davis formations (Cambrian), southeastern Missouri: Journal of Sedimentary Research, 60(4), 549–562. https://doi.org/10.1306/212F91E2-2B24-11D7-8648000102C1865D

Gregg, J.M., Sibley, D.F., 1984, Epigenetic dolomitization and the origin of xenotopic dolomite texture: Journal of Sedimentary Research, 54, 908–931. https://doi.org/10.1306/212F8535-2B24-11D7-8648000102C1865D

Hashmie, A., Rostamnejad, A., Nikbakht, F., Ghorbanie, M., Rezaie, P., Gholamalian, H., 2016, Depositional environments and sequence stratigraphy of the Bahram Formation (middle-late Devonian) in north of Kerman, south-central Iran: Geoscience Frontiers, 7(5), 821–834. https://doi.org/10.1016/j.gsf.2015.07.002

Hassani, M.J., Ameri, H., Honarmand, M., Hosseinipour, F., 2020, The microfacies, sequence stratigraphy and Genesis of the Upper Devonian phosphorites in the north of Kerman, SE Iran: Rivista Italiana di Paleontologia e Stratigrafia, 126(3), 847–864. https://doi.org/10.13130/2039-4942/14468

Hine, A.C., 1977, Lily Bank, Bahamas: history of an active oolite sand shoal: Journal of Sedimentary Research, 47, 1544–1581. https://doi.org/10.1306/212F73B5-2B24-11D7-8648000102C1865D

Hoseinabadi, M., Mahboubi, A., Shabestari, G.M., Motamed, A., 2016, Depositional environment, diagenesis, and geochemistry of Devonian Bahram formation carbonates, Eastern Iran: Arabian Journal of Geosciences, 9, 1–25. https://doi.org/10.1007/s12517-015-2056-4

Huang, J., Li, Y., Kershaw, S., Guo, W., Liang, K., Qie, W., 2022, Biostromal unit from the Middle Devonian Jinbaoshi Formation, Sichuan, Southwest China: Implications for ecological structure of coeval reef communities: Palaeogeography, Palaeoclimatology, Palaeoecology, 608, 111272. https://doi.org/10.1016/j.palaeo.2022.111272

Husince, A., Sokac, B., 2006, Early Cretaceous benthic associations (foraminifera and calcareous algae) of a shallow tropical-water platform environment (Mljet Island, southern Croatia): Cretaceous Research, 27, 418–441. https://doi.org/10.1016/j.cretres.2005.07.008

Isaacson, P.E., Curran, H.A., 1981, Anatomy of an Early Devonian carbonate buildup, central New York: Journal of Paleontology, 55(6), 1225–1236.

Joachimski, M.M., Breisig, S., Buggisch, W., Talent, J.A., Mawson, R., Gereke, M., Morrow, J.R., Day, J., Weddige, K., 2009, Devonian climate and reef evolution: insights from oxygen isotopes in apatite: Earth and Planetary Science Letters, 284(3–4). 599–609. https://doi.org/10.1016/j.epsl.2009.05.028

Johnson, A.W., Shelton, K.L., Greeg, M.J., Somerville, I.D., Wright, W.R., Nagy, Z.R., 2009, Regional studies of dolomites and their included fluids: recognizing multiple chemically distinct fluids during the complex diagenetic history of Lower Carboniferous (Mississipian) rocks of the Irish Zn-Pb ore field: Mineralogy and Petrology, 96, 1–18. https://doi.org/10.1007/s00710-008-0038-x

Königshof, P., Kershaw, S., 2006, Growth forms and palaeoenvironmental interpretation of stromatoporoids in a Middle Devonian reef, southern Morocco (west Sahara): Facies, 52, 299–306. https://doi.org/10.1007/s10347-005-0041-1

Königshof, P., Carmichael, S.K., Waters, J., Jansen, U., Bahrami, A., Boncheva, I., Yazdi, M., 2017, Palaeoenvironmental study of the Palaeotethys Ocean: the Givetian-Frasnian boundary of a shallow-marine environment using combined facies analysis and geochemistry (Zefreh Section/Central Iran): Palaeobiodiversity and Palaeoenvironments, 97, 517–540. https://doi.org/10.1007/s12549-016-0253-0

Lasemi, Y., Ghomashi, M., Amin-Rasouli, H., Kheradmand, A., 2008, The lower Triassic Sorkh shale formation of the Tabas block, east central Iran: succession of a failed-rift basin at the paleotethys margin: Carbonates and Evaporites, 23, 21–38. https://doi.org/10.1007/BF03176249

Lasemi, Y., Jahani, D., Amin-Rasouli, H., Lasemi, Z., 2012, Ancient carbonate tidalites, in Davis, R.A., Dalrymple, R.W. (eds.), Principle of tidal Sedimentology: Dordrecht, Springer, 567–607.

Lubeseder, S., Redfern, J., Boutib, L., 2009, Mixed siliciclastic-carbonate shelf sedimentation—Lower Devonian sequences of the SW Anti-Atlas, Morocco: Sedimentary Geology, 215(1-4), 13–32. https://doi.org/10.1016/j.sedgeo.2008.12.005

MacNeil, A.J., Jones, B., 2016, Stromatoporoid

http://dx.doi.org/10.18268/BSGM2025v77n2a060625

growth forms and Devonian reef fabrics in the Upper Devonian Alexandra Reef System, Canada–Insight on the challenges of applying Devonian reef facies models: Sedimentology, 63(6), 1425–1457. https://doi.org/10.1111/sed.12268

Mahmoudi, F., Mirab Shabestari, Gh., Khazaei, A.R., 2015, Sedimentary environment, diagenesis and geochemistry of carbonate rocks of Bahram Formation (Middle-Late Devonian) in Qaleh-bala section (Ozbak-kuh, east of Iran): Sedimentary facies, 8(1), 107–128.

Mount, J.F., 1984, Mixing of siliciclastic and carbonate sediments in shallow shelf environments: Geology, 12, 432–435. https://doi.org/10.1130/0091-7613(1984)12<432:MOSACS>2.0.CO;2

Mount, J.F., 1985, Mixed siliciclastic and carbonate sediments: a proposed first-order textural and compositional classification: Sedimentology, 32, 435–442. https://doi.org/10.1111/j.1365-3091.1985.tb00522.x

Nichols, G., 2023, Sedimentology and Stratigraphy: Chichester, Wiley-Blackwell, 544 p.

Parcha, S.K., Pandey, S., 2011, Devonian Ichnofossils from the Farakah Muth Section of the Pin Valley, Spiti Himalaya: Journal of the Geological Society of India, 78, 263–270. https://doi.org/10.1007/s12594-011-0082-8

Pellegrini, A.F.A., Soja, C., Minjin, C., 2012, Post-tectonic limitations on Early Devonian (Emsian) reef development in the Gobi-Altai region, Mongolia: Lethaia, 45(1), 46–61. https://doi.org/10.1111/j.1502-3931.2011.00292.x

Pohler, S.M.L., 1998, Devonian carbonate buildup facies in an intra-oceanic island arc (Tamworth Belt, New South-Wales, Australia): Facies, 39, 1–34. https://doi.org/10.1007/BF02537009

Rahiminejad, A.H., Zand-Moghadam, H., 2018, Synsedimentary formation of ooidal ironstone: an example from the Jurassic deposits of SE central Iran: Ore Geology Reviews, 95, 238–257. https://doi.org/10.1016/j.oregeorev.2018.02.028

Reineck, H.E., Singh, I.B., 1975, Depositional Sedimentary Environments: New York, Springer-Verlag, 439 p.

Salehi, M.A., Bahrami, A., Moharrami, S., Vaziri-Moghaddam, H., Pakzad, H.R., Shakeri, B., 2020, Palaeoenvironmental and sequence-stratigraphic analysis of the Middle-Late Devonian carbonates (Bahram Formation) of Anarak, western Central Iran: Journal of African Earth Sciences, 171, 103938. https://doi.org/10.1016/j.jafrearsci.2020.103938

Schlager, W., 2005, Carbonate Sedimentology and Sequence Stratigraphy: Tulsa, Oklahoma, Society for Sedimentary Geology, 208 p.

Scotese, C.R., 2014, Atlas of Devonian paleogeographic maps, PALEOMAP atlas for ArcGIS, volume 4, the late Paleozoic, maps 65–72. Evanston, IL: Mollweide Projection PALEOMAP Project.

Scotese, C.R., Mckerrow, W.S., 1990, Revised world maps and introduction, in Mckerrow, W.S., Scotese, C.R. (eds.), Palaeozoic Palaeogeography and Biogeography: London, Geological Society, Memoirs, 12, 1–21.

Seilacher, A., 1964, Biogenic sedimentary structures, in Imbrie, J., Newell, N.D. (eds.), Approaches to Paleoecology: New York, John Willey and Sons, 296–316.

Shinn, E.A., 1983, Tidal flat environment, in Scholle, P.A., Bebout, D.G., Moore, C.H. (eds.), Carbonate Depositional Environments: Tulsa, American Association Petroleum Geologists Memoir, 173–210.

Shinn, E.A., 1986, Modern Carbonate Tidal Flats: Their Diagnostic Features: Colorado School of Mines Quarterly, 81, 7–35.

Sorci, A., Cirilli, S., Spina, A., Ghorbani, M., Rettori, R., 2023, Facies analysis and depositional environment of a late Cambrian

mixed carbonate-siliciclastic ramp from the Zard Kuh Mountain (Zagros Basin, south-western Iran): Sedimentary Geology, 449, 106370. https://doi.org/10.1016/j.sedgeo.2023.106370

Stöcklin, J., 1968, Structural history and tectonics of Iran: a review: American Association of Petroleum Geologists Bulletin, 52, 1229–1258. https://doi.org/10.1306/5D25C4A5-16C1-11D7-8645000102C1865D

Stöcklin, J., 1974, Possible ancient continental margins in Iran, in Burk, C.A., Drake, C.L. (eds.), The Geology of Continental Margins: Berlin and Heidelberg, Springer-Verlag, 873–887.

Stöcklin, J., 1977, Structural correlation of the Alpine ranges between Devonian-lower carboniferous of Iran and central Asia: Mémoires hors Série de la Societe Geologique de France, 8, 333–353.

Takin, M., 1972, Iranian geology and continental drift in the Middle East: Nature, 235, 147–150. https://doi.org/10.1038/235147a0

Tamasovych, A., 2004, Microfacies and depositional environment of upper Triassic intra-platform carbonate basin; the fatric unit of west Carpathians (Slovakia): Facies, 50, 77–105. https://doi.org/10.1007/s10347-004-0004-y

Tucker, M., Wright, P., 1990, Carbonate Sedimentology: Oxford, Blackwell, 482 p.

Vahdati-Daneshmand, F., Mosavvari, F., Mahmudi Gharai, M.H., Ghasemi, A., 1995, Geological map of Zarand, 1:100,000: Tehran, Iran, Geology Survey of Iran, sheet 7351.

Vaziri, S.H., Fürsich, F.T., Kohansal-Ghadimvand, N., 2012, Facies analysis and depositional environments of the Upper Cretaceous Sadr unit in the Nakhlak area, Central Iran: Revista Mexicana de Ciencias Geológicas, 29(2), 384–397.

Warren, J.K., 2000, Dolomite, Occurrence, evolution and economical important association: Earth Science Review, 52, 1–180. https://doi.org/10.1016/S0012-8252(00)00022-2

Warren, J.K., 2006, Evaporites: Sediments, Resources and Hydrocarbons: Berlin and Heidelberg, Springer-Verlag, 1035 p.

Wei, X.J., Li, Z.X., Ma, Y.S., Li, Y.F., Hu, J.J., Liu, K., Fang, X.X., 2021, Sedimentology and sequence stratigraphy of the mixed clastic-carbonate deposits in the Late Paleozoic icehouse period: A case study from the northern Qaidam Basin: China Geology, 4(4), 673–685. https://doi.org/10.31035/cg2021068

Wendt, J., Hayer, J., Bavandpur, A.K., 1997, Stratigraphy and depositional environment of Devonian sediments in northeast and east-central Iran: Neues Jahrbuch für Geologie und Paläontologie-Abhandlungen, 206(3), 277–322. https://doi.org/10.1127/njgpa/206/1997/277

Wendt, J., Kaufmann, B., Bełka, Z., Farsan, N., Karimi Bavandpur, A., 2002, Devonian/lower carboniferous stratigraphy, facies patterns and palaeogeography of Iran. Part I. Southeastern Iran: Acta Geologica Polonica, 52(2), 129–168.

Wendt, J., Kaufmann, B., Belka, Z., Farsan, N., Karimi Bavandpour, A., 2005, Devonian/Lower Carboniferous stratigraphy, facies patterns and palaeogeography of Iran. Part II, Northern and central Iran: Acta Geologica Polonica, 55, 31–97.

Wilmsen, M., Fürsich, F.T., Seyed-Emami, K., Majidifard, M.R., 2009, An overview of the stratigraphy and facies development of the Jurassic System on the Tabas Block, east-central Iran, in Brunet, M.F., Wilmsen, M., Granath, J.W. (eds.), South Caspian to central Iran basins: London, Geological Society, Special Publications, 312(1), 323–343. https://doi.org/10.1144/SP312.15

Wilson, J.L., 1975, Carbonate facies in Geological history: Berlin, Heidelberg, Springer-Verlag, 471 p.

Wilson, M.E.J., Lokier, S.W., 2002,

http://dx.doi.org/10.18268/BSGM2025v77n2a060625

Siliciclastic and volcaniclastic influences on equatorial carbonates: insights from the Neogene of Indonesia: Sedimentology, 49, 583–601. https://doi.org/10.1046/j.1365-3091.2002.00463.x

Zamani, F., Yazdi, M., Bahrami, A., Girard, C., Spalletta, C., Ameri, H., 2021, Middle Givetian to late Famennian (Middle to Late Devonian) conodonts from the northern margin of Gondwana (Kerman region, Central Iran): Historical Biology, 33(11); 2591–2609. https://doi.org/10.1080/08912963.2020.1819997

Zand-Moghadam, H., Moussavi-Harami, R., Mahboubi, A., 2014, Sequence stratigraphy of the Early–Middle devonian succession (Padeha Formation) in Tabas Block, East-Central Iran: implication for mixed tidal flat deposits: Palaeoworld, 23(1), 31–49. https://doi.org/10.1016/j.palwor.2013.06.002

Zapalski, M.K., Baird, A.H., Bridge, T., Jakubowicz, M., Daniell, J., 2021, Unusual shallow water Devonian coral community from Queensland and its recent analogues from the inshore Great Barrier Reef: Coral Reefs, 40(2), 417–431. https://doi.org/10.1007/s00338-020-02048-9

Zecchin, M., Catuneanu, O., 2017, High-resolution sequence stratigraphy of clastic shelves VI: Mixed siliciclastic-carbonate systems: Marine and Petroleum Geology, 88, 712–723. https://doi.org/10.1016/j.marpetgeo.2017.09.012